Heterogeneous Basic Catalysis

Hideshi Hattori

Center for Advanced Research of Energy Technology (CARET), Hokkaido University, Kita-Ku, Kita 13, Nishi 8, Sapporo 060, Japan

Contents

Hideshi Hattori was born on Dec 18, 1939 in Tokyo, Japan. He graduated from the Tokyo Institute of Technology in 1963, and received a Ph.D. in engineering in 1968, whereupon he began his academic career at the Department of Chemistry, Hokkaido University. In 1971–1973, he did post-doctoral work at Rice University. He then moved to the Graduate School of Environmental Earth Science, Hokkaido University, and is presently a Professor at the Center for Advanced Research of Energy Technology, Hokkaido University. His special field of interest is solid acid and base catalysis.

I. Introduction

Acid and base are paired concepts; a number of chemical interactions have been understood in terms of acid–base interaction. Among chemical reactions which involve acid–base interactions are acid-catalyzed and base-catalyzed reactions which are initiated by acid–base interactions followed by catalytic cycles. In acid-catalyzed reactions, reactants act as bases toward catalysts which act as acids. In base-catalyzed reactions, on the contrary, reactants act as acids toward catalysts which act as bases.

In homogeneous systems, a huge number of acid-catalyzed reactions and base-catalyzed reactions are known. In heterogeneous systems, a limited number of reactions are recognized as acid- or base-catalyzed reactions. In particular, base-catalyzed reactions have been studied to a lesser extent as compared to acid-catalyzed reactions in heterogeneous systems.

Heterogeneous acid catalysis attracted much attention primarily because heterogeneous acidic catalysts act as catalysts in petroleum refinery and are known as a main catalyst in the cracking process which is the largest process among the industrial chemical processes. Extensive studies of heterogeneous cracking catalysts undertaken in the 1950s revealed that the essential nature of cracking catalysts are acidic, and generation of acidic sites on the solids was extensively studied. As a result, amorphous silica–alumina was utilized as a cracking catalyst, and then crystalline aluminosilicate (zeolite) was used afterward.

In contrast to these extensive studies of heterogeneous acidic catalysts, fewer efforts have been given to the study of heterogeneous basic catalysts. The first study of heterogeneous basic catalysts, that sodium metal dispersed on alumina acted as an effective catalyst for double bond migration of alkenes, was reported by Pines et al.[1] Considering the strong tendency of Na to donate electrons, it seems natural that Na dispersed on alumina acts as a heterogeneous basic catalyst.

Table 1. Types of Heterogeneous Basic Catalysts

(1) single component metal oxides
    alkaline earth oxides
    alkali metal oxides
    rare earth oxides
    ThO_2, ZrO_2, ZnO, TiO_2
(2) zeolites
    alkali ion-exchanged zeolites
    alkali ion-added zeolites
(3) supported alkali metal ions
    alkali metal ions on alumina
    alkali metal ions on silica
    alkali metal on alkaline earth oxide
    alkali metals and alkali metal hydroxides on alumina
(4) clay minerals
    hydrotalcite
    chrysotile
    sepiolite
(5) non-oxide
    KF supported on alumina
    lanthanide imide and nitride on zeolite

Following the report by Pines et al., certain metal oxides with a single component were found to act as heterogeneous basic catalysts in the absence of such alkali metals as Na and K. In the 1970s, Kokes et al. reported that hydrogen molecules were adsorbed on zinc oxide by acid—base interaction to form proton and hydride on the surface.[2,3] They proved that the heterolytically dissociated hydrogens act as intermediates for alkene hydrogenation. In the same period, Hattori et al. reported that calcium oxide and magnesium oxide exhibited high activities for 1-butene isomerization if the catalysts were pretreated under proper conditions such as high temperature and high vacuum.[4] The 1-butene isomerization over calcium oxide and magnesium oxide was recognized as a base-catalyzed reaction in which the reaction was initiated by abstraction of a proton from 1-butene by the basic site on the catalyst surfaces.

The catalytic activities of basic zeolites were reported also in early 1970s. Yashima et al. reported that side chain alkylation of toluene was catalyzed by alkali ion-exchanged X and Y type zeolites.[5] The reaction is a typical base-catalyzed reaction, and the activity varied with the type of exchanged alkali cation and with type of zeolite, suggesting that the basic properties can be controlled by selecting the exchanged cation and the type of zeolite.

In addition to the above mentioned catalysts, a number of materials have been reported to act as heterogeneous basic catalysts. The types of heterogeneous basic catalysts are listed in Table 1. Except for non-oxide catalysts, the basic sites are believed to be surface O atoms. Oxygen atoms existing on any materials may act as basic sites because any O atoms would be able to interact attractively with a proton. The materials listed in Table 1 act as a base toward most of the reagents and, therefore, are called heterogeneous basic catalysts or solid base catalysts.

Four reasons for recognizing certain materials as heterogeneous basic catalysts are as follows.

(1) Characterization of the surfaces indicates the existence of basic sites: Characterizations of the surfaces by various methods such as color change of the acid—base indicators adsorbed, surface reactions, adsorption of acidic molecules, and spectroscopies (UV, IR, XPS, ESR, etc.) indicate that basic sites exist on the surfaces.

(2) There is a parallel relation between catalytic activity and the amount and/or strength of the basic sites: The catalytic activities correlate well with the amount of basic sites or with the strength of the basic sites measured by various methods. Also, the active sites are poisoned by acidic molecules such as HCl, H_2O, and CO_2.

(3) The material has similar activities to those of homogeneous basic catalysts for "base-catalyzed reactions" well-known in homogeneous systems: There are a number of reactions known as base-catalyzed reactions in homogeneous systems. Certain solid materials also catalyze these reactions to give the same products. The reaction mechanisms occurring on the surfaces are suggested to be essentially the same as those in homogeneous basic solutions.

(4) There are indications of anionic intermediates participating in the reactions: Mechanistic studies of the reactions, product distributions, and spectroscopic observations of the species adsorbed on certain materials indicate that anionic intermediates are involved in the reactions.

The studies of heterogeneous catalysis have been continuous and progressed steadily. They have never been reviewed in the *Chemical Reviews* before. It is more useful and informative to describe the studies of heterogeneous basic catalysis performed for a long period. In the present article, therefore, the cited papers are not restricted to those published recently, but include those published for the last 25 years.

II. Generation of Basic Sites

One of the reasons why the studies of heterogeneous basic catalysts are not as extensive as those of heterogeneous acidic catalysts seems to be the requirement for severe pretreatment conditions for active basic catalysts. The materials which are now known as strong basic materials used to be regarded as inert catalysts. In the long distant past, the catalysts were pretreated normally at relatively low temperatures of around 723 K. The surfaces should be covered with carbon dioxide, water, oxygen, etc. and showed no activities for base-catalyzed reactions. Generation of basic sites requires high-temperature pretreatment to remove carbon dioxide, water, and, in some cases, oxygen.

This can be understood with the data in Figure 1 in which decomposition pressures are plotted against reciprocal temperature for carbonates and peroxides of alkaline earth elements.[6] In addition to carbonates and peroxides, hydroxides are formed at the surface layers of the oxides. The decomposition pressures are very low at room temperature. On exposure to the atmosphere, alkaline earth oxides adsorb carbon dioxide, water, and oxygen to form carbonates, hydroxides, and peroxides. Removal of the adsorbed species from the surfaces is essential to reveal the oxide surfaces. Therefore, high-temperature pretreatment is required to obtain the metal oxide surfaces.

The evolutions of water, carbon dioxide, and oxygen when $Mg(OH)_2$ and BaO are heated under vacuum at elevated temperatures are shown in Figures 2 and
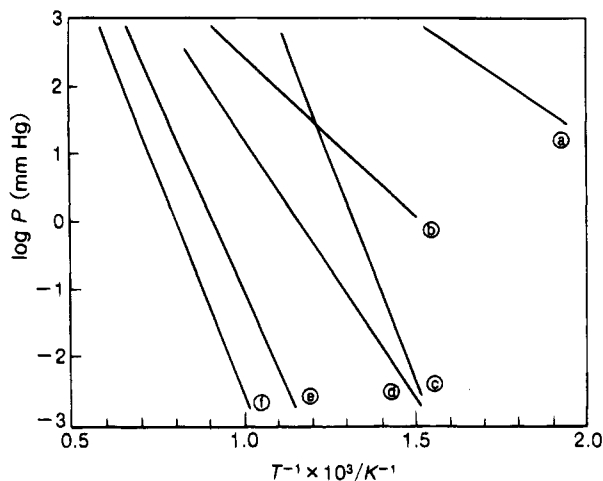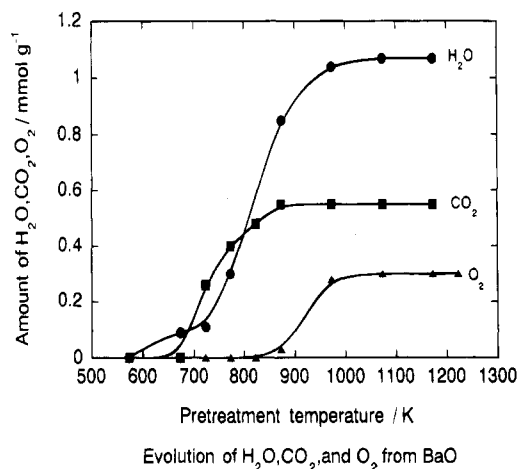
Figure 1. Equilibrium pressure for decomposition:

(a) $2SrO_2 \rightleftharpoons 2SrO + O_2$, (b) $2BaO_2 \rightleftharpoons 2BaO + O_2$,

(c) $MgCO_3 \rightleftharpoons MgO + CO_2$, (d) $CaCO_3 \rightleftharpoons CaO + CO_2$,

(e) $SrCO_3 \rightleftharpoons SrO + CO_2$, (f) $BaCO_3 \rightleftharpoons BaO + CO_2$.

Evolution of H_2O and CO_2 from $Mg(OH)_2$
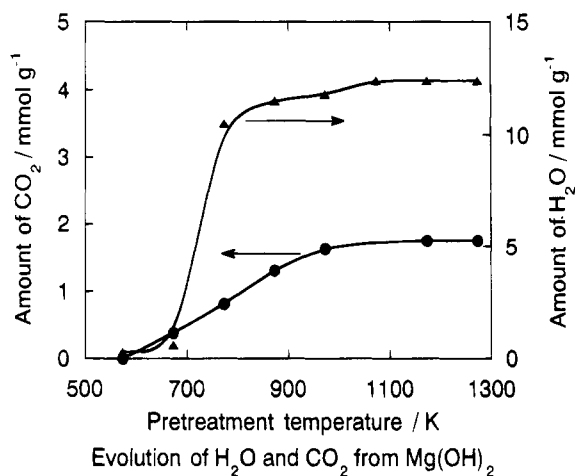
Figure 2. Evolution of H_2O and CO_2 from $Mg(OH)_2$.

Evolution of H_2O, CO_2, and O_2 from BaO

Figure 3. Evolution of H_2O, CO_2, and O_2 from BaO.

$3.^{4,7}$ For MgO, evolution of water and carbon dioxide continues up to 800 K. For BaO, evolution of these gases continues to much higher temperatures. In addition, oxygen evolves above 900 K. Evolution of carbon dioxide, water, and oxygen results in generation of basic sites on the surfaces which act as
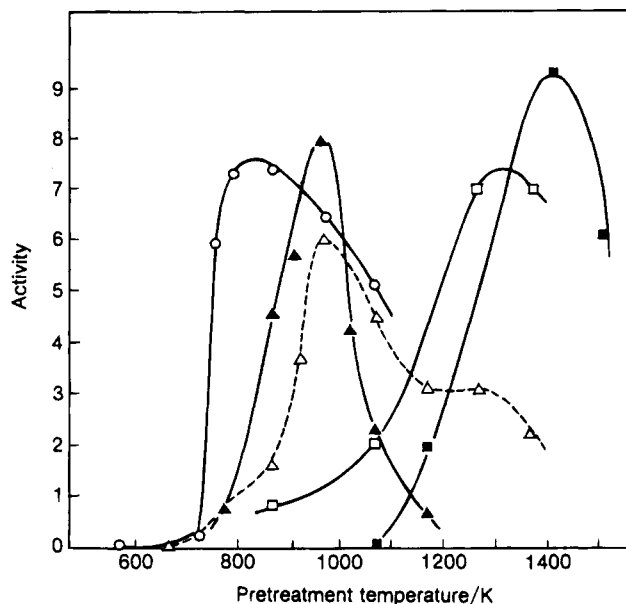

Figure 4. Variations of activity of MgO for different types of reactions as a function of pretreatment temperature: O, 1-butene isomerization at 303 K $(3.5 \times 10^3$ mmHg min^{-1} g^{-1}) ▲, CH_4-D_2 exchange at 673 K $(4.3 \times 10^3\%$ s^{-1} g^{-1}); △, amination of 1,3-butadiene with dimethylamine at 273 K $(5 \times 10^{17}$ molecules min^{-1} g^{-1}); □, 1,3-butadiene hydrogenation at 273 K $(2.5 \times 10\%$ min^{-1} g^{-1}); ■, ethylene hydrogenation at 523 K $(0.3\%$ min^{-1} g^{-1}).

catalytically active sites for several reaction types.

The nature of the basic sites generated by removing the molecules covering the surfaces depends on the severity of the pretreatment. The changes in the nature of basic sites are reflected in the variations of the catalytic activities as a function of pretreatment temperature. In many cases, the variations of the activity are dissimilar for different reaction types. The activity variations of MgO for different reactions are shown in Figure 4.[8] The activity maxima appear at different catalyst-pretreatment temperatures for different reaction types: 800 K for 1-butene isomerization, 973 K for methane−D_2 exchange and amination of 1,3-butadiene with dimethylamine, 1273 K for hydrogenation of 1,3-butadiene, and 1373 K for hydrogenation of ethylene.

As the pretreatment temperature increases, the molecules covering the surfaces are successively desorbed according to the strength of the interaction with the surface sites. The molecules weakly interacting with the surfaces are desorbed at lower pretreatment temperatures, and those strongly interacting are desorbed at higher temperatures. The sites that appeared on the surfaces by pretreatment at low temperatures are suggested to be different from those that appeared at high temperatures. If simple desorption of molecules occurs during pretreatment, the basic sites that appeared at high temperatures should be strong. However, rearrangement of surface and bulk atoms also occurs during pretreatment in addition to the desorption of the molecules, which is evidenced by a decrease in the surface area with an increase in the pretreatment temperature.

Coluccia and Tench proposed a surface model for MgO (Figure 5).[9] There exist several Mg−O ion pairs of different coordination numbers. Ion pairs of low
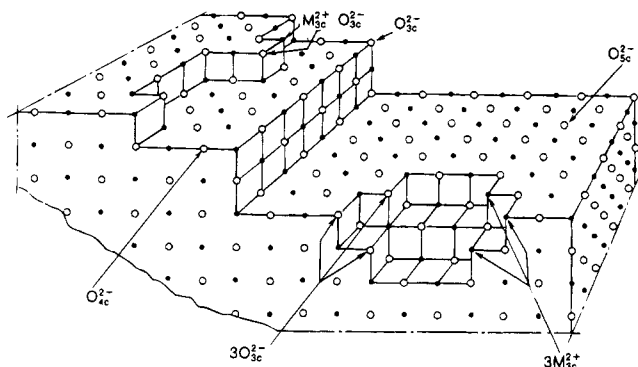
Figure 5. Ions in low coordination on the surface of MgO. (Reprinted from ref 9. Copyright 1981 Kodansha.)

coordination numbers exist at corners, edges, or high Miller index surfaces of the (100) plane. Different basic sites generated by increasing the pretreatment temperature appear to correspond to the ion pairs of different coordination numbers. However, the correspondence between the catalytically active sites for different reaction types and the coordination number of the ion pairs is not definite yet.

Among the ion pairs of different coordination numbers, the ion pair of 3-fold Mg^{2+}–3-fold O^{2-} (Mg^{2+}_{3c}–O^{2-}_{3c}) is most reactive and adsorbs carbon dioxide most strongly. To reveal the ion pair Mg^{2+}_{3c}–O^{2-}_{3c}, the highest pretreatment temperature is required. At the same time, the ion pair Mg^{2+}_{3c}–O^{2-}_{3c} is most unstable. The Mg^{2+}_{3c} and O^{2-}_{3c} tend to rearrange easily at high temperature. The appearance of such highly unsaturates sites by the removal of carbon dioxide and the elimination by the surface atom rearrangement compete. Such competition results in the activity maxima as the pretreatment temperature is increased.

Although the surface model shown in Figure 5 is proposed for MgO, the other metal oxide heterogeneous bases may be in a situation similar to that of MgO. The nature of basic sites varies with the severity of the pretreatment conditions for most heterogeneous basic catalysts.

The surface sites generated on rare earth oxides, however, behave differently from those of the other heterogeneous base catalysts. The sites of rare earth oxides do not seem to vary in nature with pretreatment temperature. Variations of the activities of La_2O_3 as a function of the pretreatment temperature is shown in Figure 6 for 1-butene isomerization, 1,3-butadiene hydrogenation, and methane–D_2 exchange.[10-12] Pretreatment at 923 K results in the maximum activity for all reactions. The surface sites generated by removal of water and carbon dioxide seem to be rather homogeneous in the sense that the same surface sites are relevant to all the reactions mentioned above.

III. Characterization of Basic Surfaces

The surface properties of the heterogeneous basic catalysts have been studied by various methods by which existence of basic sites has been realized. Different characterization methods give different information about the surface properties. All the properties of basic sites cannot be measured by any
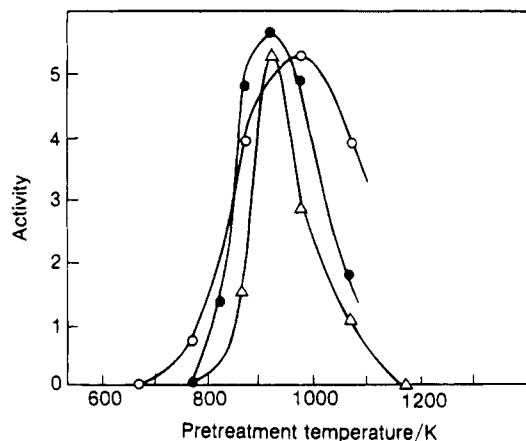
Figure 6. Variations of activity of La_2O_3 for different types of reaction as a function of pretreatment temperature: O, 1-butene isomerization at 303 K (1 unit: 6.4 × 10^{20} molecules min^{-1} g^{-1}); △, CH_4–D_2 exchange at 573 K (1 unit: 10^{-2}% s^{-1} g^{-1}); ●, 1,3-butadiene hydrogenation at 273 K (1 unit: 1.2 × 10^{20} molecules min^{-1} g^{-1}).

single method. Integration of the results obtained by different characterizations leads us to understand the structures, reactivities, strengths, and amounts of the basic sites on the surfaces. In this section, representative methods for characterization of the surface basic sites are described. It is emphasized what aspect of the basic sites is disclosed by each characterization method.

III-1. Indicator Methods

Acid–base indicators change their colors according to the strength of the surface sites and pK_{BH} values of the indicators. The strength of the surface sites are expressed by an acidity function (H_-) proposed by Paul and Long. The H_- function is defined by the following equation:[13,14]

$$H_- = pK_{BH} + \log [B^-]/[BH]$$

where [BH] and [B$^-$] are, respectively, the concentration of the indicator BH and its conjugated base, and pK_{BH} is the logarithm of the dissociation constant of BH. The reaction of the indicator BH with the basic site ($\underline{B}$) is

$$BH + \underline{B} = B^- + \underline{B}H^+$$

The amount of basic sites of different strengths can be measured by titration with benzoic acid. A sample is suspended in a nonpolar solvent and an indicator is adsorbed on the sample in its conjugated base form. The benzoic acid titer is a measure of the amount of basic sites having a basic strength corresponding to the pK_{BH} value of the indicator used. Using this method, Take et al. measured outgassed samples of MgO, CaO, and SrO. The results are shown in Figure 7.[15] Magnesium oxide and CaO possess basic sites stronger than $H_- = 26$.

The indicator method can express the strength of basic sites in a definite scale of H_-, but this has disadvantages too. Although the color change is assumed to be the result of an acid–base reaction, an indicator may change its color by reactions different from an acid–base reaction. In addition, it
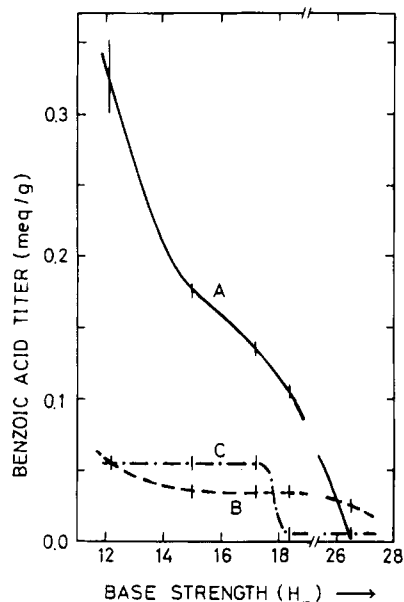
Figure 7. Benzoic acid titer vs base strength of (A) MgO, (B) CaO, and (C) SrO. (Reprinted from ref 15. Copyright 1971 Academic.)

requires a long time for benzoic acid to reach an adsorption equilibrium when titration is carried out in a solution. In some cases, the surface of heterogeneous basic catalysts may dissolve into a titration solution. If this happens, the number of basic sites should be overestimated. Therefore, special care should be taken with the indicator method.

## III-2. Temperature-Programmed Desorption (TPD) of Carbon Dioxide

This method is frequently used to measure the number and strength of basic sites. The strength and amount of basic sites are reflected in the desorption temperature and the peak area, respectively, in a TPD plot. However, it is difficult to express the strength in a definite scale and to count the number of sites quantitatively. Relative strengths and relative numbers of basic sites on the different catalysts can be estimated by carrying out the TPD experiments under the same conditions. If the TPD plot gives a sharp peak, the heat of adsorption can be estimated.

TPD plots of carbon dioxide desorbed from alkaline earth oxides are compared in Figure 8 in which adsorption of carbon dioxide and the following treatment before the TPD run were done under the same conditions.[16] The strength of basic sites is in the increasing order of MgO < CaO < SrO < BaO. The number of basic sites per unit weight that can retain carbon dioxide under the adsorption conditions increases in the order BaO < SrO < MgO < CaO.

Enhancement of basic strength by addition of alkali ions to X-zeolite in excess of the ion exchange capacity was demonstrated by TPD plots of carbon dioxide as shown in Figure 9.[17] The peak areas are larger for the alkali ion-added zeolites (solid lines) than for the ion-exchanged zeolites (dotted lines). In particular, desorption of carbon dioxide still continues at the desorption temperature of 673 K for ion-added zeolites.
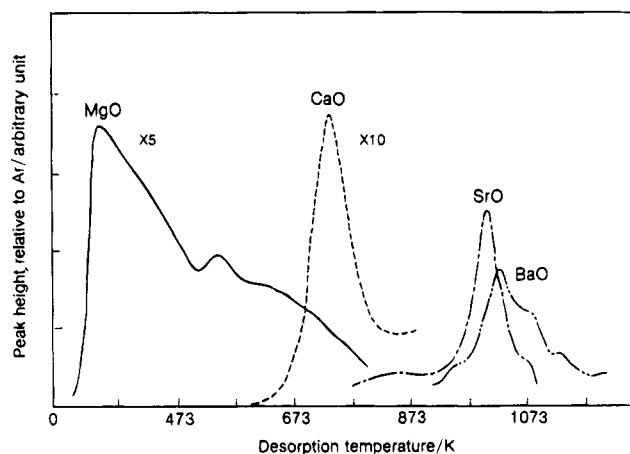
Figure 8. TPD plots of carbon dioxide desorbed from alkaline earth oxides. (Reprinted from ref 16. Copyright 1988 Elsevier.)
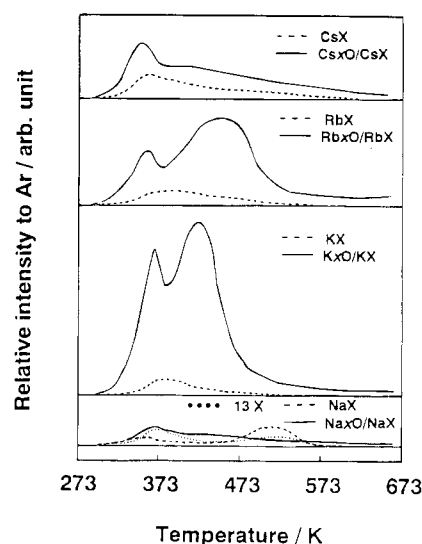

Figure 9. TPD plots of CO_2 adsorbed on alkali ion-exchanged and alkali ion-added zeolites.

III-3. UV Absorption and Luminescence Spectroscopies

UV absorption and luminescence spectroscopies give information about the coordination states of the surface atoms.

High surface area MgO absorbs UV light and emits luminescence, which is not observed with MgO single crystal. Nelson and Hale first observed the absorption at 5.7 eV, which is lower than the band gap (8.7 eV, 163 nm) for bulk MgO by 3 eV.[18] Tench and Pott observed photoluminescence.[19,20] The UV absorption corresponds to the following electron transfer process involving surface ion pair.[21,22]

$$Mg^{2+}O^{2-} + h\nu \rightarrow Mg^{+}O^{-}$$
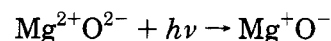
Absorption bands were observed at 230 and 274 nm, which are considerably lower in energy than the band at 163 nm for bulk ion pairs. The bands at 230 and 274 nm are assigned to be due to the surface O^{2-} ions of coordination numbers 4 and 3, respectively.

Luminescence corresponds to the reverse process of UV absorption, and the shape of the luminescence spectrum varies with the excitation light frequency
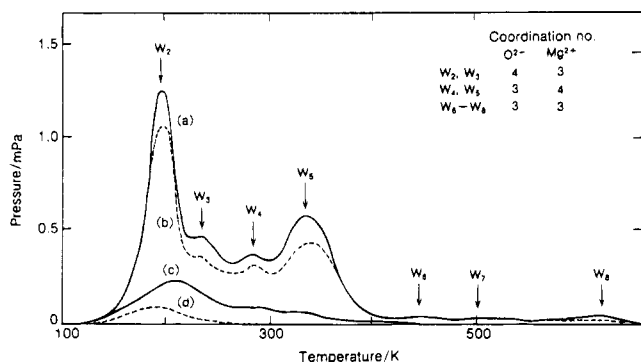
Figure 10. TPD plots for hydrogen adsorbed on MgO at various pretreatment temperatures/K: (a) 1123, (b) 973, (c) 823, (d) 673.

and with the adsorpion of molecules. Emission sites and excitation sites are not necessarily the same. Excitons move on the surface and emit at the ion pair of low coordination numbers where emission efficiency is high.

Ion pairs of low coordination numbers responsible for UV absorption and luminescence exist at corners, edges, or high Miller index surfaces. The surface model for MgO shown in figure 5 was proposed on the basis of UV absorption and luminescence together with the effects of hydrogen adsorption on the luminescence spectrum. The luminescence spectrum excited by the 274 nm light was much more severely influenced by hydrogen adsorption than that excited by the 230 nm light. Hydrogen molecules interact more strongly with the ion pairs of coordination number 3 than with those of coordination number 4. Hydrogen molecules are heterolytically dissociated on these sites.

Although the UV absorption and luminescence spectroscopies give us useful information about the coordination state, it is difficult to count the number of the sites of a certain coordination state.
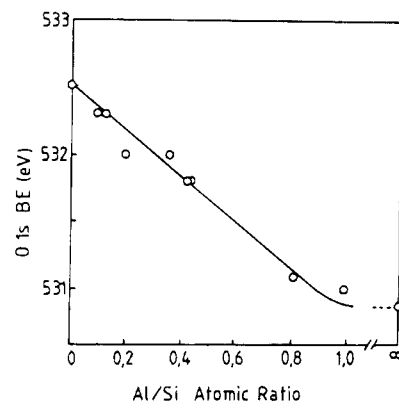
III-4. Temperature-Programmed Desorption of Hydrogen

This method gives information about the coordination state of the surface ion pairs when combined with the other methods such as UV absorption and luminescence spectroscopies. The number of each ion pair could be counted if TPD is accurately measured with a proper calibration method. This method has been applied only to the MgO surface.

Hydrogen is heterolytically dissociated on the surface of MgO to form H^+ and H^-, which are adsorbed on the surface O^{2-} ion and Mg^{2+} ion, respectively. TPD plots of hydrogen adsorbed on MgO pretreated at different temperatures are shown in Figure 10.[23,24] Seven desorption peaks appear in the temperature range 200−650 K, and appearance of the peaks varies with the pretreatment temperature. Appearance of the peaks at different temperatures indicates that several types of ion pairs with different coordination numbers exist on the surface of MgO. The adsorption sites on MgO pretreated at different temperatures and the coordination numbers of each ion pair are assigned as summarized in Table 2. The assignment of the surface ion pairs are based on the surface structure model of MgO (Figure 5).

Table 2. Coordination Numbers of Active Sites on MgO and Their Concentration Obtained from TPD for Hydrogen Adsorbed

| active site | coordination no. | | number of sites/10^{15} m^{-2} at pretreatment temperature | | | |
	O_{1C}	Mg_{LC}	673 K	823 K	973 K	1123 K
W_2 and W_3	4	3	4.0	11.6	29.3	32.4
W_4 and W_5	3	4	0.0	4.9	22.1	26.5
W_6 and W_7	3	3	0.0	0.3	1.3	4.1
W_8	3	3			1.2	4.2

Figure 11. Correlation between the binding energy of the O_{1s} band and the Al/Si atomic ratio. (Reprinted from ref 25. Copyright 1988 Academic.)

TPD of hydrogen supports the surface model of MgO illustrated.

Heterolytic dissociation of hydrogen on the MgO surface is also demonstrated by IR spectroscopy. The IR bands for O−H and Mg−H stretching vibration were observed.[9]

III-5. XPS

The XPS binding energy (BE) for oxygen reflects the basic strength of the oxygen. As the O_{1s} BE decreases, electron pair donation becomes stronger. Okamoto et al. studied the effects of zeolite composition and the type of cation on the BE of the constituent elements for X- and Y-zeolites ion-exchanged with a series of alkali cations as well as H-forms of A, X, Y, and mordenite.[25] The BE values of O_{1s} are plotted against the Al/Si atomic ratio in Figure 11. The BE of O_{1s} decreases as the Al content increases.

The effect of an ion-exchanged cation on the O_{1s} BE is shown in Figure 12 as a function of the electronegativity (x) of the cation. With increasing x, the O_{1s} BE increases. The O_{1s} BE of zeolite is directly delineated to the electron density of the framework oxygen. On the basis of XPS features of zeolite, Okamoto et al. proposed a bonding model of zeolite as shown in Figure 13.[25] Configurations I and II are in resonance. In configuration I, extra framework cations form covalent bonds with framework oxygens, while in configuration II, the cations form fully ionic bondings with the negatively charged zeolite lattice. As the electronegativity of the cation increases and approaches that of oxygen, the contribution of configuration I increases to reduce the net charges on the lattice. This explains the dependences of the O_{1s} BE on the electronegativity of the cation as shown in Figure 12.
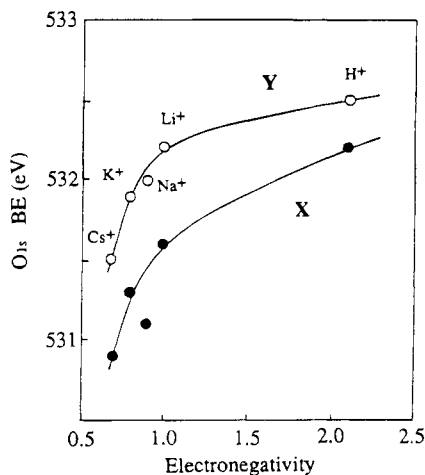
Figure 12. Binding energy of the O_{1s} band for cation exchanged zeolite as a function of the cation electronegativity (x): (●) Y-zeolite and (○) X-zeolites. (Reprinted from ref 25. Copyright 1988 Academic.)
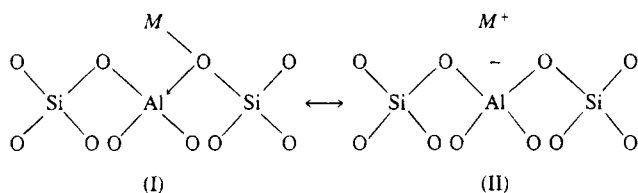

Figure 13. Schematic bonding model of zeolite.

Although the relation between electron density and the basic strength of O is not theoretically established, a good correlation between the BE of the N_{1s} band and basicity is well established for a wide variety of organic compounds containing N. It may be acceptable that the BE of the O_{1s} band changes monotonously with the basic strength of O when comparison is made within a same series of exchanged cations.

XPS measurement of the probe molecule adsorbed on basic sites gives information about the strength of the basic sites. Huang et al. measured the N_{1s} BE of the pyrrole adsorbed on alkali cation-exchanged X- and Y-zeolites.[26] The N_{1s} envelopes were deconvoluted into three peaks. One of the peaks was assigned to pyrrole adsorbed on the framework oxygen adjacent to the alkali cations other than the sodium cation. The BE of the peak varies with the exchanged cation in such a way that the N_{1s} BE decreases as the basic strength of the zeolite increases as Li < Na < K < Rb < Cs. The deconvolution of XPS N_{1s} peaks into three peaks indicates that the basic strength of the framework oxygen is inhomogeneous in the zeolite cage and that the cation exerts an influence only on the adjacent framework atoms. These suggest that electrons are localized significantly on $M^+(AlO_2)^-$ units. A proposed model for pyrrole chemisorbed on a basic site of alkali cation-exchanged zeolite is shown in Figure 14.

As described later, the basic strength is reflected in the N–H stretching vibration frequency of pyrrole in the IR spectrum.[27] The N_{1s} BE in XPS correlates linearly with the N–H vibration frequencies of chemisorbed pyrrole. As the exchanged cation changes in the sequence Li, Na, K, Rb, and Cs, both the N_{1s} BE and the frequency of the N–H stretching vibration decrease for X- and Y-zeolites.[26]
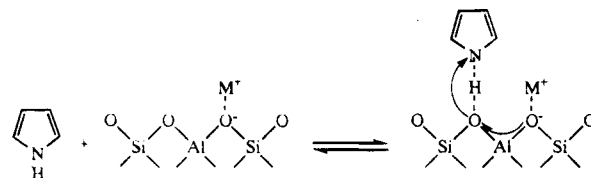
Figure 14. Model for pyrrole chemisorbed on a basic site.

Scheme 1. Adsorbed Forms of Carbon Dioxide

bidentate   unidentate
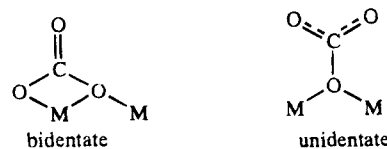
III-6. IR of Carbon Dioxide

This method gives information about the adsorbed state of CO_2 on the surface. Carbon dioxide interacts strongly with a basic site and, therefore, the surface structures including basic sites are estimated from the adsorbed state of CO_2.

Carbon dioxide is adsorbed on heterogeneous basic catalysts in different forms: bidentate carbonate, unidentate carbonate, and bicarbonate (Scheme 1). On the MgO surface, the adsorbed form varies with the coverage of the adsorbed carbon dioxide. Bidentate carbonate is dominate at low coverage, and unidentate carbonate at high coverage.[28] Evans and Whately reported the adsorption of carbon dioxide on MgO.[29] In addition to unidentate and bidentate carbonates, bicarbonate species were also detected. For CaO, carbon dioxide is adsorbed in the form of bidentate carbonate regardless of the coverage.

In the adsorption state of unidentate carbonate, only surface oxygen atoms participate, while the metal ion should participate in the adsorption state of bidentate. In other words, the existence of only a basic site is sufficient for unidentate carbonate, but the existence of both a basic site and a metal cation is required for bidentate carbonate.

III-7. IR of Pyrrole

Pyrrole is proposed to be a probe molecule for measurement of the strength of basic sites.[17] The IR band ascribed to the N–H stretching vibration shifts to a lower wavenumber on interaction of the H atom in pyrrole with a basic site. Barthomeuf measured the shifts of N–H vibration of pyrrole adsorbed on alkali ion exchanged zeolites.[27,30] The results are given in Table 3. The charges on the oxygen calculated from Sanderson's electronegativities are also listed in Table 3. The shift increases when the negative charge on the oxide ion increases. The negative charge is associated closely with the strength of the basic site. The basic strengths of alkali ion-exchanged zeolites are in the order CsX > NaX > KY > NaY, KL, Na-mordenite, Na-beta.

The N–H vibration frequencies observed by IR are plotted against the N_{1s} BE observed by XPS as shown in Figure 15.[26] For both X- and Y-zeolites, linear relations are observed; strengths of the basic sites

Table 3. Shifts of N—H Vibration of Pyrrole Adsorbed on Zeolites and Calculated Average Charge on Oxygen

zeolite	$\Delta\nu_{NH}{}^a$	$q_0{}^b$	zeolite	$\Delta\nu_{NH}{}^a$	$q_0{}^b$
CsX	240	−0.461	Na-MOR	30	−0.278
NaX	180	−0.413	Na-beta	30	−0.240
KY	70	−0.383	Cs ZSM-5	0	−0.236
NaY	30−40	−0.352	Na ZSM-5	0	−0.225
KL	30	−0.356			

^{a} Shift of N—H from the liquid. ^{b} Charge on oxygen calculated from Sanderson electronegativity.

ν_{NH}

cm^{-1}
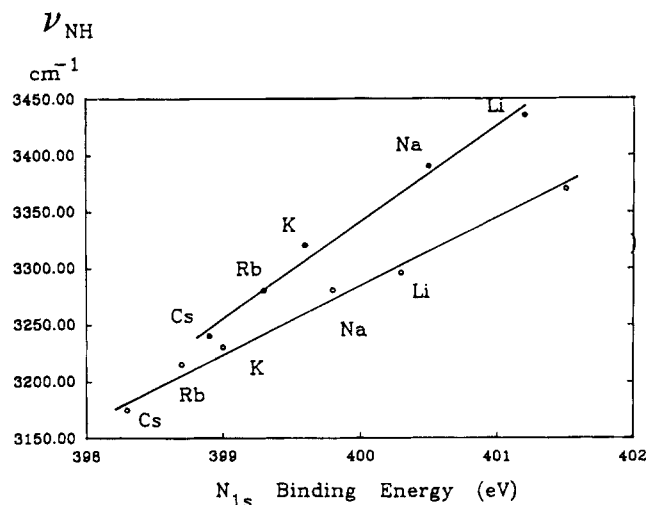
Figure 15. Relationship between N_{1s} binding energy and N—H stretching vibration frequencies of chemisorbed pyrrole on (○) X-zeolites and (●) Y-zeolites. (Reprinted from ref 26. Copyright 1992 Academic.)

are in the order CsX > RbX > KK X NaX > LiX and CsY > RbY > KY > NaY > LiY.

## III-8. Oxygen Exchange between Carbon Dioxide and Surface

This method gives information about the dynamic nature of interaction of adsorbed CO_2 with the surface ion pair. As described above, carbon dioxide is used as a probe molecule for the basic properties in IR and TPD. If ^{18}O-labeled, carbon dioxide is used, additional information about the nature of basic sites is obtained.

Yanagisawa et al. reported that oxygen exchange between adsorbed CO_2 and the MgO surface takes place to a considerable extent.[31] They observed a TPD desorption peak consisting mainly of $C^{16}O_2$ and $C^{16}O^{18}O$ after $C^{18}O_2$ adsorption on MgO and suggested that the adsorbed $C^{18}O_2$ interacts with the peroxy ion ($^{16}O_s)_2{}^{2-}$ on a defect in the MgO surface. Essentially the same result was independently reported by Shishido et al.[32] The interpretation of the exchange mechanisms, however, was not the same as that of Yanagisawa et al.

Tsuji et al. reported the oxygen exchange in detail.[33] TPD plots for $C^{18}O_2$ adsorbed on MgO are shown in Figure 16 in which 41×10^{-6} mol $C^{18}O_2$ g^{-1} (one CO_2 molecule per 670 Å^2) was adsorbed. Extensive oxygen exchange was observed; no $C^{18}O_2$ was desorbed. Proposed processes for the mechanism of migration of the surface bidentate carbonate are shown in Figure 17. There are at least two ways,
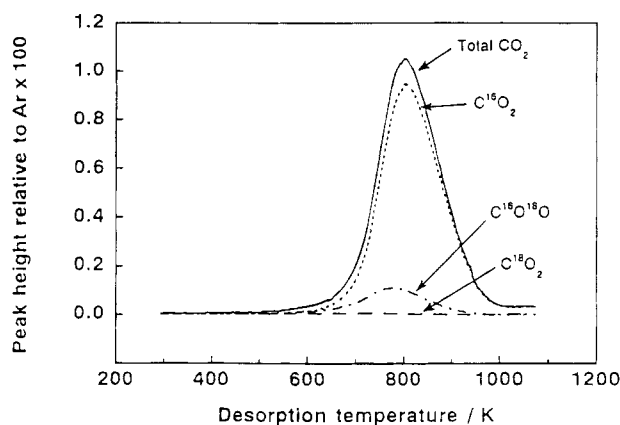
Figure 16. TPD plots for $C^{18}O_2$ adsorbed on MgO.
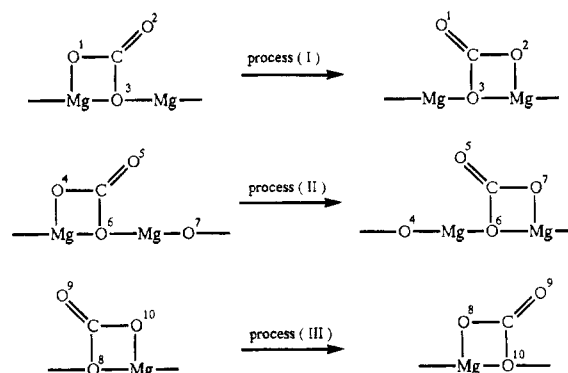
Figure 17. Proposed processes for the mechanisms of migration of the surface bidentate carbonate.

processes I and II, for the adsorbed carbonate species to migrate over the surface. In process I, carbon dioxide rolls over the surface in such a way that the free oxygen atom in the bidentate carbonate approaches the adjacent Mg atom on the surface. In process II, the carbon atom approaches the adjacent O atom on the surface.

In process I, the carbonate species always contains two ^{18}O atoms. Therefore, repetition of process I results in the exchange of one oxygen atom, but not the exchange of two oxygen atoms in the desorbed CO_2. The repetition of process II also results in the exchange of one oxygen atom. For evolution of $C^{16}O_2$, both processes I and II should be involved. In addition to processes I and II, process III is possible. This process is essentially the same as the mechanism proposed for the oxygen exchange between bidentate carbonate and oxide surface. The carbonate species are able to migrate on the surface over a long distance by a combination of process I-III without leaving the surface, if process III exists. IR spectra of the adsorbed CO_2 changes with increasing temperature. It is suggested that the bidentate carbonate formed on room temperature adsorption of CO_2 migrates over the surface as the temperature is raised in the TPD run. The migration occurs mostly in the temperature range from room temperature to 473 K.

The results of the oxygen exchange between CO_2 and MgO surface suggest an important aspect of the nature of surface basic sites. The basic sites are not fixed on the surface but are able to move over the surface when carbon dioxide is adsorbed and de-

Scheme 2. 1-Butene Isomerization

cis-2-butene

$CH_2=CH-CH_2-CH_3$

1-butene

trans-2-butene
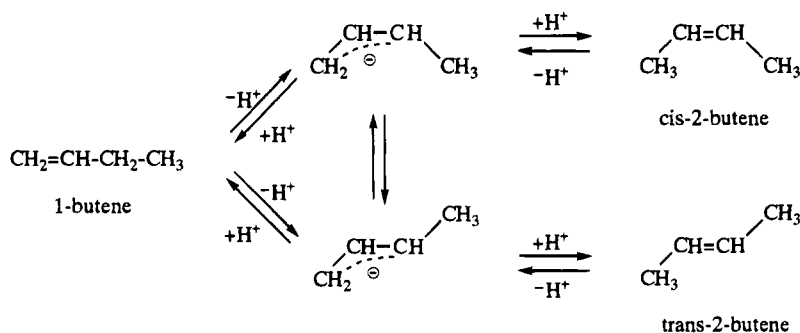
sorbed. The position of the basic site (surface O atom) changes as CO_2 migrate over the basic site. In addition, it became clear that not only O^{2-} basic sites but also adjacent Mg^{2+} sites participate in CO_2 adsorption. Therefore, it is reasonable to consider that the metal cations adjacent to the basic site participate in the base-catalyzed reactions.

IV. Catalysis by Heterogeneous Basic Catalysts

In this section, selected examples of heterogeneous base-catalyzed reactions are described. Some of them aim at elucidating the reaction mechanisms. The others are applications to various organic syntheses to show the potential use of heterogeneous catalysts.

IV-1. Double Bond Migration

1-Butene isomerization to 2-butenes has been extensively studied over many heterogeneous basic catalysts to elucitade the reaction mechanisms and to characterize the surface basic properties. The reaction proceeds at room temperature or below over most of heterogeneous basic catalysts. Over MgO, for example, the reaction occurs even at 223 K if the catalyst is properly activated.

The reaction mechanisms for 1-butene isomerization are shown in Scheme 2.[34]

The reaction is initiated by abstraction of allylic H by basic sites to form cis or trans forms of the allyl anion. In the form of the allyl anion, the cis form is more stable than the trans form. Therefore, cis-2-butene is predominantly formed at the initial stage of the reaction. A high cis/trans ratio observed for the base-catalyzed isomerization is in contrast to the value close to unity for acid-catalyzed isomerization.

The cis to trans ratio in 2-butenes produced could be used to judge whether the reaction is a base-catalyzed or acid-catalyzed one. Tsuchiya measured the ratio cis/trans in 1-butene isomerization, and found a high value for Rb_2O.[35]

Coisomerization of butene-d_0 and -d_8 is a useful method to determine the reaction mechanisms.[36] In the coisomerization, a mixture containing equal amounts of nondeuteriobutene (d_0) and perdeuterio-butene (d_8) is allowed to react, and the isotopic distributions in the products and reactant are analyzed. If the reaction proceeds by hydrogen addition—abstraction mechanisms, an intermolecular H (or D) transfer is involved and the products will be composed of d_0, d_1, d_7, and d_8 isotopic species. On the other hand, if the reaction proceeds by hydrogen abstraction—addition mechanisms, an intramolecular

H (or D) transfer is involved, and the products will be composed of d_0 and d_8 isotopic species.

Since an H^+ is abstracted first for base-catalyzed isomerization to form allyl anions to which the H^+ returns at a different C atom, an intramolecular H (or D) transfer is expected. Therefore, an intramolecular H (or D) transfer and a high cis/trans ratio are characteristic features for 1-butene double bond isomerization over heterogeneous basic catalysts.[37,38]

The fundamental studies of 1-butene double bond isomerization over heterogeneous basic catalysts were extended to the double bond migration of olefins having more complex structures such as pinene (1), carene (2), protoilludene (4), illudadiene (5), as shown below.[39-41]
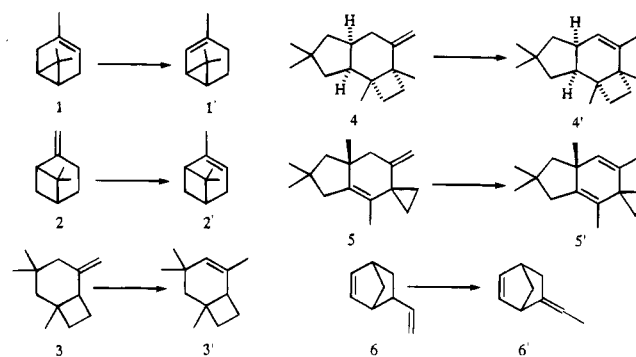
These olefins contain three-membered and four-membered rings. If acidic catalysts were used, the ring-opening reactions would easily occur, and the selectivities for double bond migration should markedly decrease. A characteristic feature of heterogeneous basic catalysts is a lack of $C-C$ bond cleavage ability. The double bond migration selectively occurs without $C-C$ bond cleavages over heterogeneous basic catalysts.

As mentioned above, the heterogeneous basic catalysts are highly active for double bond migration, the reactions proceed at a low temperature. This is advantageous for olefins which are unstable at high temperature. Because of this advantage, the heterogeneous basic catalyst, $Na/NaOH/Al_2O_3$, is used for an industrial process for the selective double bond migration of 5-vinylbicyclo[2.2.1]heptene (6).[41,42] The reaction proceeds at the low temperature of 243 K.

Heterogeneous basic catalysts have another advantage in double bond migration. For the double bond migration of unsaturated compounds containing heteroatoms such as N and O, heterogeneous basic catalysts are more efficient than acidic catalysts.

Scheme 3. Double Bond Migration of Allylamines to Enamines
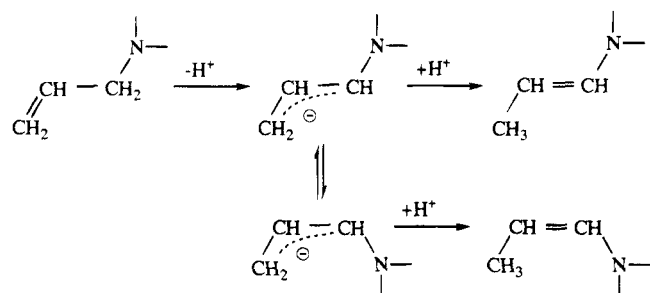
Acidic catalysts interact strongly with heteroatoms, became poisoned, and show no activity. On the other hand, the active sites of heterogeneous basic catalysts interact weakly with heteroatoms and, therefore, act as efficient catalysts.
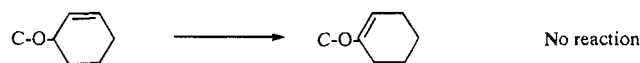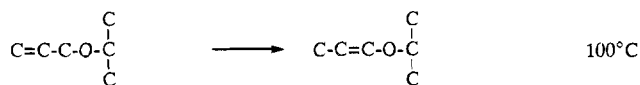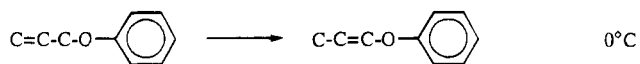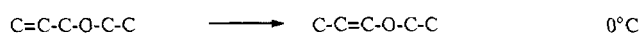
Allylamines undergo double bond migration to enamines over alkaline earth oxides (Scheme 3).[43] For instance, 1-N-pyrrolidino-2-propene isomerizes to 1-N-pyrrolidino-1-propene over MgO, CaO, SrO, and BaO at 313 K. The reaction mechanisms are essentially the same as those for 1-butene isomerization. The basic sites abstract an H$^+$ from the reactant to form allyl anions as an intermediate as shown below. In this scheme too, the cis-form of the intermediate of the allyl anion is more stable than the trans-form, and the products are mostly in the thermodynamically less stable cis-form.

Similarly, 2-propenyl ethers undergo double bond migration to 1-propenyl ethers.[44] The reaction mechanisms are the same as those for 1-butene and allylamines in the sense that the intermediates are allyl anions and mostly in the cis-form. Among heterogeneous basic catalysts, CaO exhibits the highest activity, and La$_2$O$_3$, SrO, and MgO also show high activities. The reaction temperatures required to initiate the reactions are different for each reactant, as shown below. 3-Methoxycyclohexene is unreac-


tive, which is explained as being due to the fact that the adsorbed state is such that the allylic H points away from the surface, and cannot be abstracted by the basic sites on the surface.

Double bond migration of safrole to isosafrole was reported to proceed at 300 K over Na/NaOH/Al$_2$O$_3$:[41]

IV-2. Dehydration and Dehydrogenation

In general, alcohols undergo dehydration to olefins and ethers over acidic catalysts, and dehydrogenation
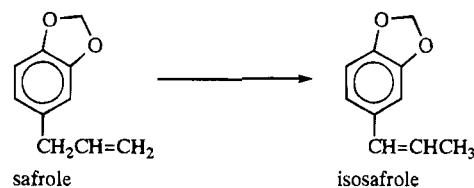
to aldehydes or ketones over basic catalysts. In some cases, however, heterogeneous basic catalysts promote dehydration of alcohols in which the mechanisms and product distribution differ from those for acid-catalyzed dehydration. The characteristic features of base-catalyzed dehydration are observed for 2-butanol dehydration. The products consist mainly of 1-butene over the rare earth oxides,[45] ThO$_2$,[46,47] and ZrO$_2$.[48] This is in contrast to the preferential formation of 2-butenes over acidic catalysts. The initial step in the base-catalyzed dehydration is the abstraction of an H$^+$ at C-1 and 2-butanol to form anion.

Dehydration of 1-cyclohexylethanol to vinylcyclohexane has been industrialized by use of ZrO$_2$ as a catalyst.[49] In the dehydration of 2-alcohols to the corresponding 1-olefins over ZrO$_2$, the selectivity for 1-olefins depends on the amount of Si contained in ZrO$_2$ as an impurity. Si contaminants in ZrO$_2$ generate acidic sites. By treatment of ZrO$_2$ with NaOH to eliminate the acidic sites, the byproducts of 2-olefins are markedly reduced and the selectivity for 1-olefins is increased. The ZrO$_2$ treated with NaOH is used for the industrial process for the production of vinylcyclohexane.
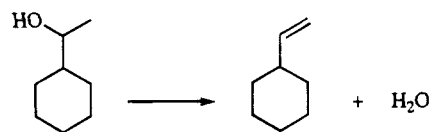
Intramolecular dehydration of monoethanolamine to ethylenimine has also been industralized by use of the mixed oxide catalyst composed of Si, alkali metal, and P. The catalyst possesses both weakly acidic and basic sites.[50] Because monoethanolamine has two strong functional groups, weak sites are sufficient to interact with the reactant. If either acidic sites or basic sites are strong, the reactant interacts too strongly with the sites and forms undesirable byproducts. It is proposed that the acidic and basic sites act cooperatively as shown in Scheme 4. The composition of the catalyst is adjusted to control the surface acidic and basic properties. A selectivity of 78.8% for ethylenimine was obtained for the catalyst composed of Si/Cs/P/O in the atomic ratio 1/0.1/0.08/2.25.

IV-3. Hydrogenation

Kokes and his co-workers studied the interaction of olefins with hydrogen on ZnO, and reported heterolytic cleavages of H$_2$ and C$-$H bonds.[2,3] The negatively charged π-allyl anions are intermediate for propylene hydrogenation. Participation of heterolytically dissociated H$^+$ and H$^-$ in the hydrogenation is generally applicable in base-catalyzed hydrogenation. The observation that MgO pretreated at 1273 K exhibited olefin hydrogenation activities was

Scheme 4. Intramolecular Dehydration of Monoethanolamine
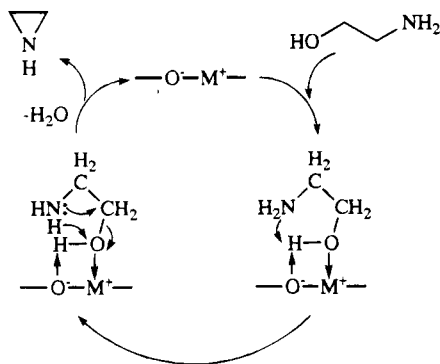
Scheme 5. Hydrogenation of 1,3-Butadiene

Scheme 6. Hydrogenation of Carbon Monoxide
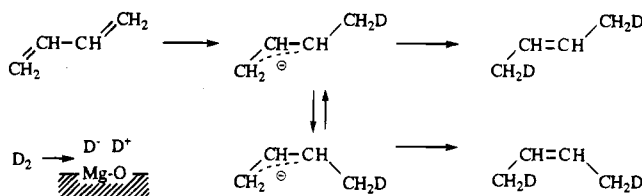
a clear demonstration of heterogeneous base-catalyzed hydrogenation.[51] The hydrogenation occurring on heterogeneous basic catalysts has characteristic features which distinguish heterogeneous basic catalysts from conventional hydrogenation catalysts such as transition metals and transition metal oxides.

The characteristic features of base-catalyzed hydrogenation are as follows.

(1) There is a large difference in the hydrogenation rate between monoenes and conjugated dienes: Conjugated dienes undergo hydrogenation much faster than monoenes. For example, 1,3-butadiene undergoes hydrogenation at 273 K over alkaline earth oxides, while butenes need a reaction temperature above 473 K. The products of diene hydrogenation consist exclusively of monoenes, with no alkanes being formed at 273 K.

(2) There is a predominant occurrence of 1,4-addition of H atoms in contrast to 1,2-addition which is commonly observed for conventional hydrogenation catalysts: In 1,3-butadiene hydrogenation, 2-butenes are preferentially formed over heterogeneous basic catalysts, while 1-butene is the main product over conventional hydrogenation catalysts.

(3) There is retention of the molecular identity of H atoms during reaction: While a hydrogen molecule dissociates on the catalyst surface, two H atoms used for hydrogenation of one reactant molecule originate from one hydrogen molecule.

Features 1 and 2 are characteristic of hydrogenation in which anionic intermediates are involved.[52] The reaction (Scheme 5) of 1,3-butadiene hydrogenation is shown below, where H is replaced by D for clarity. The products contain two D atoms at the terminal C atoms if D_2 is used instead of H_2.

Deuterium 1 is dissociatively adsorbed to form D^+ and D^-. 1,3-Butadiene consists of 93% s-trans conformer and 7% s-cis conformer in the gas phase at 273 K. At first, D^- attacks 1,3-butadiene to form the allyl anion of the trans form which undergoes either interconversion to form cis allyl anion or addition of
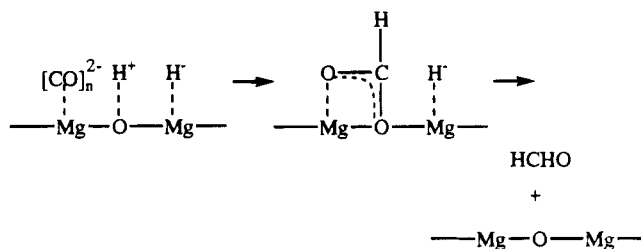
D^+ to form butenes. Since the electron density of the allyl anions is highest on the terminal C atom, the positively charged D^+ selectively adds to the terminal C atom to complete 1,4-addition of D atoms to yield 2-butene.

On alkaline earth oxides, the interconversion between the trans-allyl anion and cis-allyl anion is faster than the addition of D^+. As a result, cis-2-butene-d_2 is preferentially formed. On the other hand, the addition is faster than the interconversion on ThO_2,[53] ZrO_2,[54,55] and rare earth oxides,[56] trans-2-butene-d_2 being a main product.

A large difference in the reactivity between dienes and monoenes is caused by difficulty of alkyl anion formation compared to allyl anion formation. Alkyl anions are less stable than allyl anions; thus, the reactions of monoenes with H^- to form alkyl anions require high temperature.

Feature 3 arose from the location of the active sites. Both D^+ and D^- on one set of active sites are assumed not to migrate to other sites, and each set of active sites is isolated from the others. This happens because the basic hydrogenation catalysts are metal oxides.

The active sites for hydrogenation on alkaline earth oxides are believed to be metal cation–O^{2-} ion pairs of low coordination, as described in the preceding section. In the surface model structure of MgO, it is plausible that the Mg^{2+}_{3c}–O^{2-}_{3c} pairs act as hydrogenation sites.

Dissociatively adsorbed H^+ and H^- also hydrogenate CO on MgO, La_2O_3, ZrO_2, and ThO_2.[57,58] TPD study and IR measurement indicate that the reaction proceeds by the following mechanism shown in Scheme 6.

1,3-Butadiene undergoes transfer hydrogenation with 1,3-cyclohexadiene over La_2O_3, CaO, ThO_2, and ZrO_2.[59,60] The product distributions are similar to those for hydrogenation with H_2 except for ZrO_2, on which a relatively large amount of 1-butene is formed.

Direct hydrogenation (or reduction) of aromatic carboxylic acids to corresponding aldehydes has been industrialized by use of ZrO_2.[61,62] Although the reaction mechanism is not clear at present, the hydrogenation and dehydration abilities, which are associated with the basic properties of ZrO_2, seem to be important for promoting the reaction. The catalytic properties are improved by modification with the metal ions such as Cr^{3+} and Mn^{4+} ions. Crystallization of ZrO_2 is suppressed and coke formation is avoided by addition of the metal ions.

$$ArCOOH + H_2 \longrightarrow ArCHO + H_2O$$
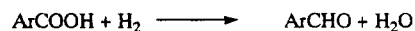
Scheme 7. Amination of 1,3-Butadiene

Scheme 8. Hydrogen Transfer from 2-Propanol to Aldehydes and Ketones
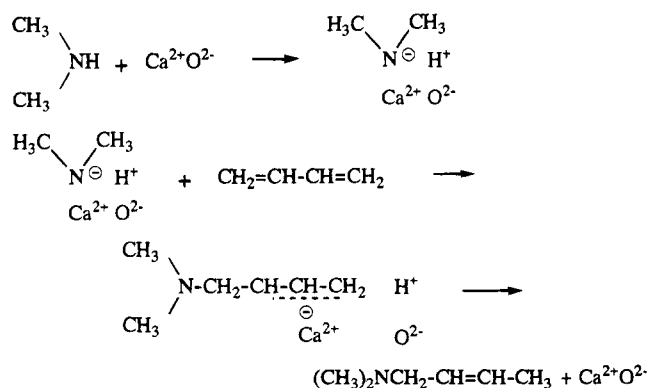
IV-4. Amination

Amines undergo an addition reaction with conjugated dienes over heterogeneous basic catalysts.[63] Primary and secondary amines add to conjugated dienes to form unsaturated secondary and tertiary amines, respectively. Amination with monoenes scarcely proceeds over basic catalysts. The reaction mechanisms for amination with conjugated dienes are essentially the same as those for the hydrogenation in the sense that heterolytic dissociation of hydrogen ($H_2 \ll H^+ + H^-$) and amine ($RNH_2 \ll H^+ + RNH^-$) are involved in the reaction. The sequence that the anion and H^+ successively add to the 1,4 position of conjugated dienes is common to hydrogenation and amination. As an example, the reaction mechanisms for addition of dimethylamine to 1,3-butadiene are shown in Scheme 7. The reaction over CaO takes place at 273 K.

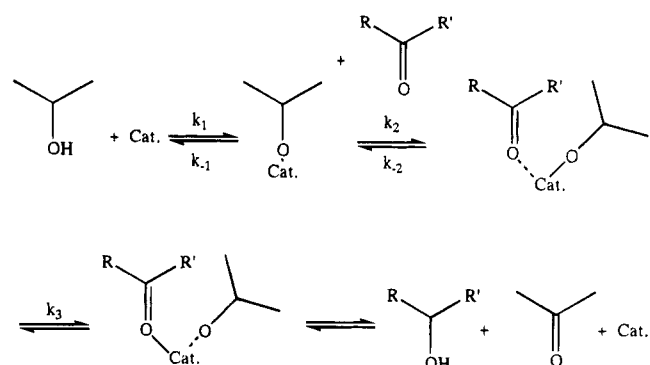## IV-5. Meerwein–Ponndorf–Verley Reduction

Meerwein–Ponndorf–Verley reduction is the hydrogenation in which alcohols are used as a source of hydrogen and is one of the hydrogen transfer reactions. Aldehyde and ketones react with alcohols to produce corresponding alcohols by Meerwein–Ponndorf–Verley reduction:

Shibagaki et al. studied Meerwein–Ponndorf–Verley reduction of various kinds of aldehydes and ketones in the temperature range 273–473 K.[64] They found hydrous zirconium oxide as a highly active catalyst for the reactions. 2-Propanol was used as a hydrogen source. On the basis of the isotope effect and kinetic analysis, it was suggested that the slow step is hydride transfer from the adsorbed 2-propanol to the adsorbed carbonyl compound (Scheme 8).

The reactions of carboxylic acids with alcohols to form esters are also catalyzed by hydrous zirconium oxide at a reaction temperature above 523 K.[65] Similarly, amidation of carboxylic acids or esters with amines or ammonia proceeds over hydrous zirconium oxide in the temperature range 423–473 K.[66]

Although hydrous zirconium oxide is proposed to be an effective catalyst for the above reactions, the

Scheme 9. Meerwein–Ponndorf–Verley Reduction of Ketones or Aldehydes with 2-Propanol
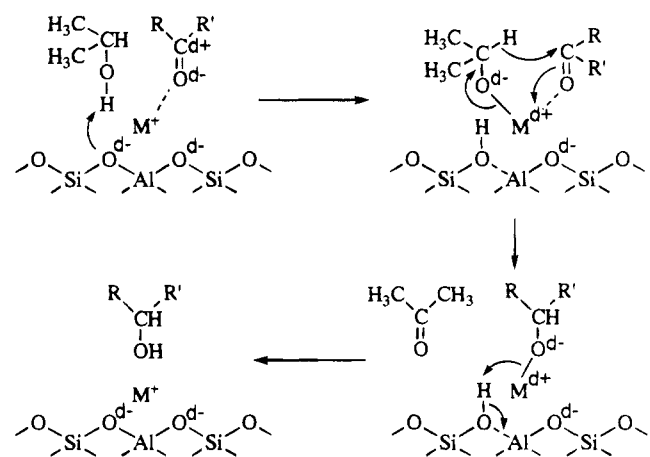
nature of the active sites has not been elucidated. The reaction mechanisms involving the active sites are not clear for the hydrous zirconium oxide catalyzed reactions. In particular, the reason why the hydrous form of zirconium oxide is more efficient than the anhydrous form of zirconium oxide is unclear.

Meerwein–Ponndorf–Verley reduction of ketones or aldehydes with 2-propanol proceeds over x-zeolites ion-exchanged with Cs^+ and Rb^+.[67] The mechanisms proposed for the zeolites are shown in Scheme 9. The reaction is initiated by abstraction of an H^+ from 2-propanol by the basic sites of the catalyst. In addition to the basic sites, exchanged cations play a role of stabilizing the ketone by the hydride transfering from adsorbed 2-propanol to the ketone.

IV-6. Dehydrocyclodimerization of Conjugated Dienes

Conjugated dienes such as 1,3-butadiene and 2-methyl-1,3-butadiene (isoprene) react over ZrO_2 and MgO to yield aromatics at 643 K.[68,69] Heterogeneous basic catalysts other than ZrO_2 and MgO scarcely exhibit appreciable activities. For the formation of aromatics from dienes, two kinds of mechanisms are possible. One involves the Diels–Alder reaction followed by double bond migration and dehydrogenation. The other involves anionic intermediates.

Over MgO, 1,3-butadiene mainly produces o- and p-xylenes, which will not be formed via the Diels–Alder reaction. Over ZrO_2, the main product from

Scheme 10. Dehydrocyclodimerization of 1,3-Butadiene
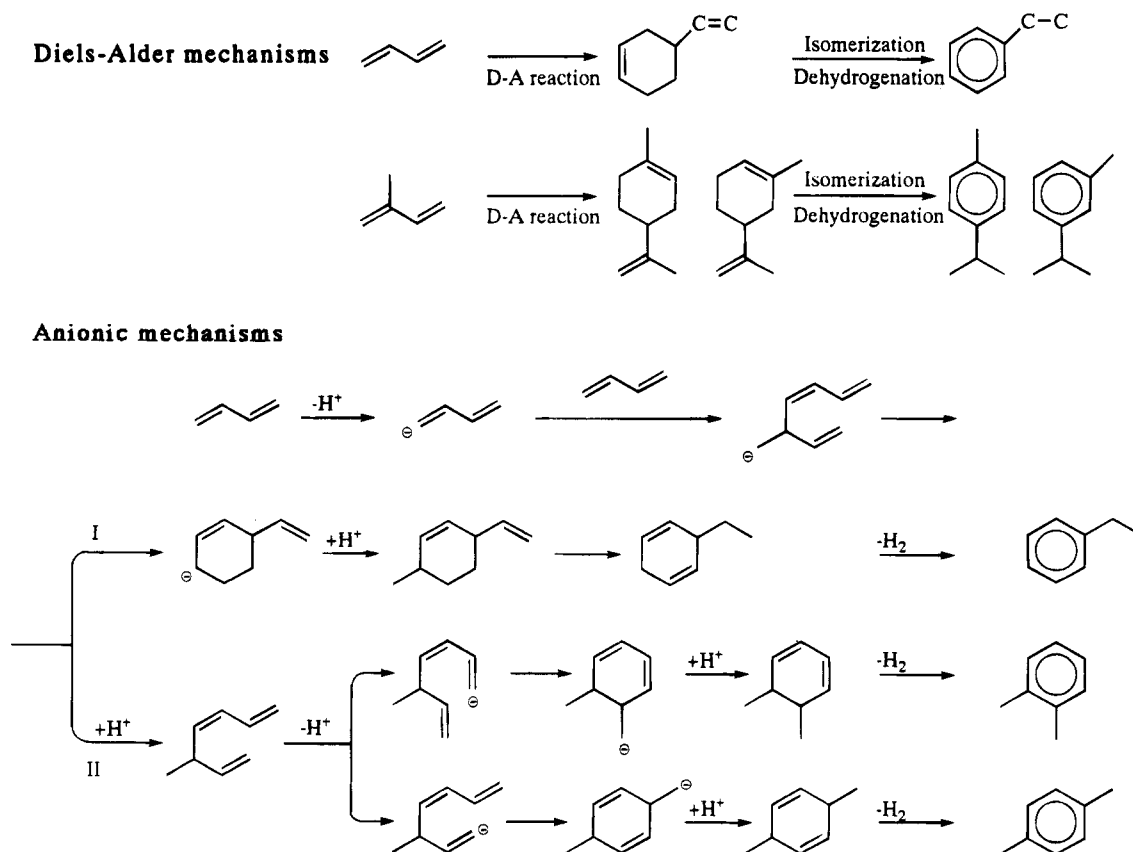
1,3-butadiene is ethylbenzene which will be formed via the Diels–Alder reaction. Two mechanisms for dehydrocyclodimerization are shown in Scheme 10. The mechanisms involving the Diels–Alder reaction take place over ZrO_2, and the anionic mechanisms take place over MgO.

IV-7. Alkylation

In general, alkylation of aromatics occurs at a ring position over an acidic catalyst, while side chain alkylation takes place over a basic catalyst. Toluene undergoes side chain alkylation with methanol to produce ethylbenzene and styrene over Cs^+ ion-exchanged X-zeolite.[5]

The first step in this reaction is dehydrogenation of methanol to formaldehyde, which undergoes aldol type reaction with toluene to form styrene. Ethylbenzene is formed by hydrogenation of styrene. The basic sites in the zeolite catalyst participate in both the dehydrogenation of methanol and the aldol type reaction.

Alkylation of toluene was studied by computer graphics on the basis of quantum chemical calculation.[70,71] The calculation also suggests that the high activity results from copresence of acidic and basic sites in a cavity of zeolite.
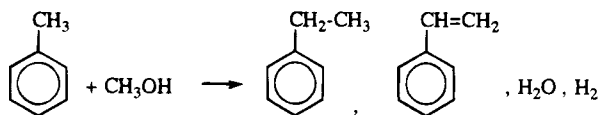
The zeolites having alkali ions in excess of their ion-exchange capacity exhibit higher activities than the simple ion-exchanged zeolites.[72] The high activities are caused by the generation of strong basic sites by addition of alkali ions which are located in the zeolite cavities in the form of alkali oxides.

$K/KOH/Al_2O_3$ is an efficient catalyst for alkylation of isopropylbenzene with olefins such as ethylene and propylene.[41] The reaction occurs at 300 K. In this reaction, too, alkylation occurs selectively at the side chain. The selective occurrence of the side chain alkylation is due to the anionic mechanisms as proposed by Suzukamo et al. The basic sites of $K/KOH/Al_2O_3$ are sufficiently strong to abstract an H^+ from isopropylbenzene to form an unstable tertiary anion at a low temperature.

IV-8. Aldol Addition and Condensation

Aldol addition of acetone to form diacetone alcohol is well known to be catalyzed by $Ba(OH)_2$. Alkaline earth oxides, La_2O_3, and ZrO_2 are also active for the reaction in the following order: BaO > SrO > CaO > MgO > La_2O_3 > ZrO_2.[73] With MgO, addition of a small amount of water increases the activity, indicating that the basic OH^- ions either retained on the surface or formed by dehydration of diacetone alcohol are active sites for aldol addition of acetone. By the tracer experiments in which a mixture containing equal amount of acetone-d_0 and -d_8 was allowed to react, the slow step was elucidated to be step B in Scheme 11.[74]

By use of the catalysts possessing both acid and base sites, the product diacetone alcohol undergoes dehydration to mesityl oxide. If hydrogenation ability is further added to the catalyst, mesityl oxide is hydrogenated to methyl isobutyl ketone (MIBK).

Scheme 11. Aldol Addition of Acetone

Step A $\quad$ CH$_3$-C-CH$_3$ + B $\longrightarrow$ CH$_3$-C-$\overset{\ominus}{C}$H$_2$ + H$^+$B
$\qquad\qquad\quad$ ‖ $\qquad\qquad\qquad\qquad$ ‖
$\qquad\qquad\quad$ O $\qquad\qquad\qquad\qquad\quad$ O

Step B $\quad$ CH$_3$-C-$\overset{\ominus}{C}$H$_2$ + $\overset{H_3C}{\underset{H_3C}{>}}$C=O $\longrightarrow$ CH$_3$-C-CH$_2$-C-O $^\ominus$
$\qquad\qquad\quad$ ‖ $\qquad\qquad\qquad\qquad\qquad\qquad$ ‖ $\qquad$ |
$\qquad\qquad\quad$ O $\qquad\qquad\qquad\qquad\qquad\qquad\quad$ O $\quad$ CH$_3$

Step C $\quad$ CH$_3$-C-CH$_2$-C-O$^\ominus$+ H$^+$B $\longrightarrow$ CH$_3$-C-CH$_2$-C-OH + B
$\qquad\qquad\quad$ ‖ $\quad$ | $\qquad\qquad\qquad\qquad\qquad$ ‖ $\qquad$ |
$\qquad\qquad\quad$ O $\quad$ CH$_3$ $\qquad\qquad\qquad\qquad\quad$ O $\quad$ CH$_3$
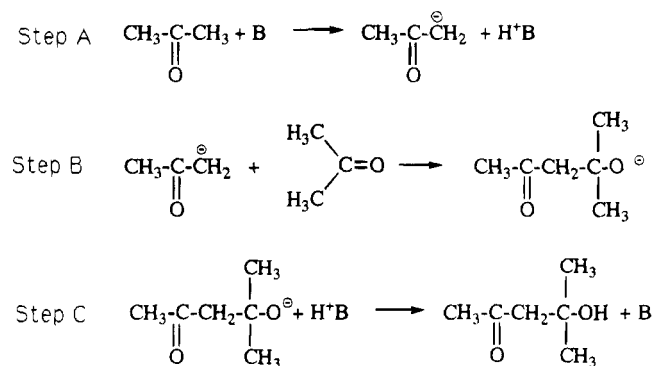
When the aldol condensation of acetone is performed over A-, X-, Y-, or L-zeolites containing alkali metal clusters at 623 K, mesityl oxide and isophorone are produced as main products.[75] The ratio of the two products is dependent on the types of zeolites. A-type zrolite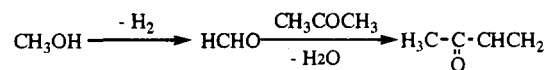s favor the formation of the smaller molecule of mesityl oxide. With X- or Y-zeolite, isophorone is preferentially produced. For the smaller pore sized L-zeolite, the formation of mesityl oxide is about twice as great as that of isophorone.[76] These catalysts possess acidic sites in addition to basic sites. Controlling the acid−base properties and choice of the zeolite pore size results in obtaining each product selectively.

Aldol condensation of formaldehyde with methyl propionate to form methyl methacrylate is catalyzed by X- and Y-zeolites having a basic property. The highest conversion was obtained with the zeolite ion-exchanged with K followed by being impregnated with potassium hydroxide.[77]
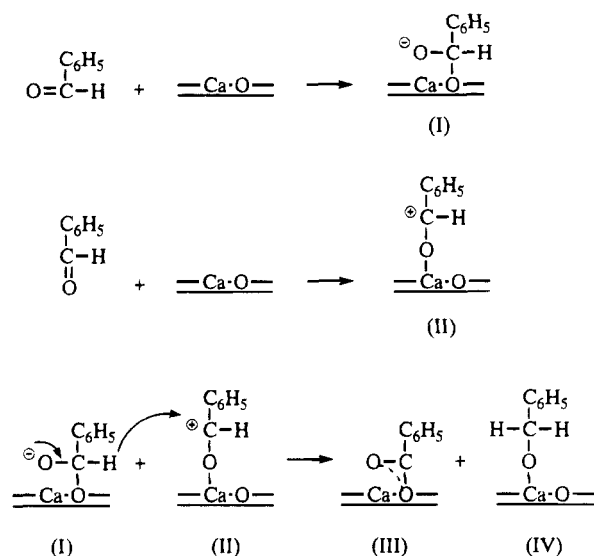
Hydrotalcite (Mg$_6$Al$_2$(OH)$_{16}$CO$_3$·4H$_2$O) and chryso-tile (Mg$_3$(OH)$_4$Si$_2$O$_5$) act as efficient catalysts for the production of methyl vinyl ketone (MVK) through aldol condensation between acetone and formaldehyde at 673 K.[78] Synthetic Co^{2+} ion-exchange chryso-tile, Co$_x$Mg$_{3-x}$(OH)$_4$Si$_2$O$_5$, produces methyl vinyl ketone from acetone and methanol. By addition of Co^{2+}, dehydrogenation sites are generated. Methanol is dehydrogenated to formaldehyde which undergoes aldol condensation with acetone to produce MVK.

CH$_3$OH $\xrightarrow{\text{- H}_2}$ HCHO $\xrightarrow[\text{- H$_2$O}]{\text{CH}_3\text{COCH}_3}$ H$_3$C-C·CHCH$_2$
$\qquad\qquad\qquad\qquad\qquad\qquad\qquad\qquad\quad$ ‖
$\qquad\qquad\qquad\qquad\qquad\qquad\qquad\qquad\quad$ O

IV-9. The Tishchenko Reaction

The Tischenko reaction is a dimerization of aldehydes to form esters. Since the reaction mechanisms are similar to those of the Cannizzaro reaction, the Tischenko reaction is through to be a base-catalyzed reaction.

Benzaldehyde converts to benzylbenzoate over alkaline earth oxides.[79] This reaction proceeds by a Tishchenko type reaction as shown in Scheme 12.

In this reaction, not only basic sites (O^{2-} ion) but also acidic sites (metal cation) participate. The slow step is H$^-$ transfer from I to II. The activities of the alkaline earth oxides were reported to be in the order MgO < CaO < SrO < BaO, indicating that basic strength is important among alkaline earth oxides.

Scheme 12. Esterification of Benzaldehyde

(I)
$\qquad$ C$_6$H$_5$ $\qquad\qquad\qquad\qquad\qquad$ C$_6$H$_5$
$\qquad$ | $\qquad\qquad\qquad\qquad\qquad$ $^\ominus$O-C-H
O=C-H $\quad$ + $\quad$ —Ca·O— $\longrightarrow$ —Ca·O—

(II)
$\qquad$ C$_6$H$_5$ $\qquad\qquad\qquad\qquad\qquad$ C$_6$H$_5$
$\qquad$ | $\qquad\qquad\qquad\qquad\qquad$ $^\oplus$C-H
$\qquad$ C-H $\qquad\qquad\qquad\qquad\qquad$ O
$\qquad$ ‖ $\quad$ + $\quad$ —Ca·O— $\longrightarrow$ —Ca·O—
$\qquad$ O

$^\ominus$O-$\overset{C_6H_5}{\underset{|}{C}}$-H $\nearrow$ $^\oplus\overset{C_6H_5}{\underset{|}{C}}$-H $\qquad$ $\overset{C_6H_5}{\underset{|}{O-C}}$ $\qquad$ $\overset{C_6H_5}{\underset{|}{H-C}}$-H
—Ca·O— $\quad$ + $\quad$ O $\longrightarrow$ —Ca·O— $\quad$ + $\quad$ O
$\qquad\qquad\qquad$ —Ca·O— $\qquad\qquad\qquad\qquad$ —Ca·O—

(I) $\qquad\qquad$ (II) $\qquad\qquad$ (III) $\qquad\qquad$ (IV)

For the aldehydes with α-hydrogen, such as benzaldehyde and pivalaldehyde, Tishchenko reactions take place selectively to produce corresponding esters. For the aldehydes having α-hydrogen, Tish-chenko reactions compete with aldol condensations. This was typically observed in the reaction of butyraldehyde.

In self-condensation of butyraldehyde, the dimers resulting from aldol condensation and the trimers resulting from Tishchenko reaction of the dimer with butyraldehyde were formed by use of alkaline earth oxides as catalysts, as shown in Scheme 13.

By use of aluminas modified with alkalis as catalysts, the reaction was selective for the formation of dimer by aldol condensation, and the Tishchenko reaction scarcely occurred. For the aldol condensation, the presence of only basic sites is sufficient, but for the Tishchenko reaction, the presence of both basic sites and acidic sites is required. By modification of alumina with alkali ions, basic sites are generated and the acidic sites are suppressed. Therefore, only the aldol condensation takes place. On the other hand, a considerable amount of trimer was formed on alkaline earth oxides. It is suggested that not only basic sites but also acidic sites participate in the reaction taking place on alkaline earth oxides.

IV-10. Michael Addition

Michael additions are conjugate additions of carbanions and are catalyzed by bases such as sodium hydroxide, sodium ethoxide, and piperidine. The reactions have special value since they serve to form carbon−carbon bonds. However, only limited types of heterogeneous catalysts have been applied to Michael additions. In heterogeneous system, the basic sites are responsible for forming the carbanion by abstraction of an H$^+$ from the molecule having an α-hydrogen.

Partially dehydrogenated Ba(OH)$_2$ catalyzes Michael additions of chalcones with active methylene compounds such as ethyl malonate, ethyl acetoacetate, acetylacetone, nitromethane, and acetophenone.[80]

Potassium fluoride supported on alumina (KF-Al$_2$O$_3$) is active for the following Michael additions

Scheme 13. Self-Condensation of Butyraldehyde
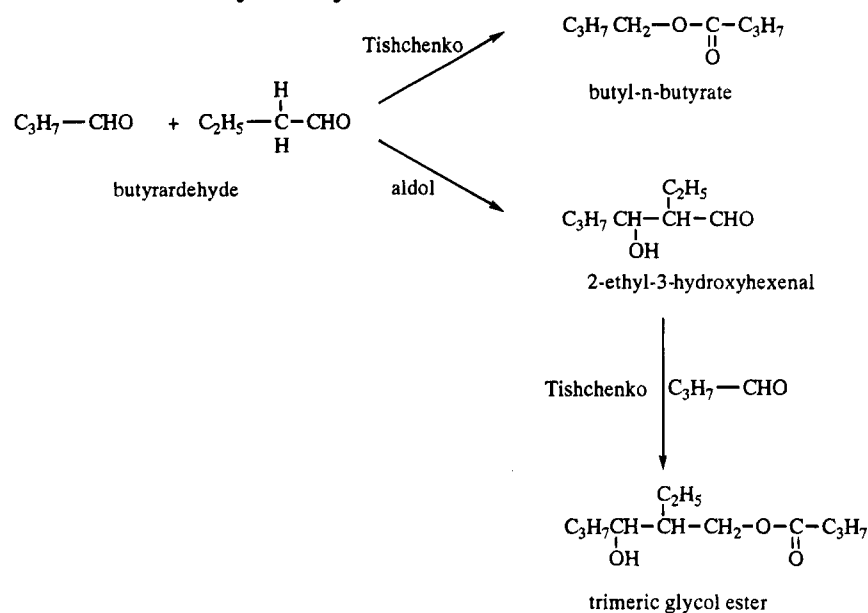
at room temperature: nitromethane with 3-buten-2-one and 1,3-diphenyl-2-propen-1-one,[81] nitroethane with 3-buten-2-one,[82] and dimenone with methyl vinyl ketone.[83]

Dimerization of methyl crotonate proceeds by self-Michael addition to form methyl diesters of (Z)- and (E)-2-ethylidene-3-methylglutalic acid (Z-MEG and E-MEG).[84]
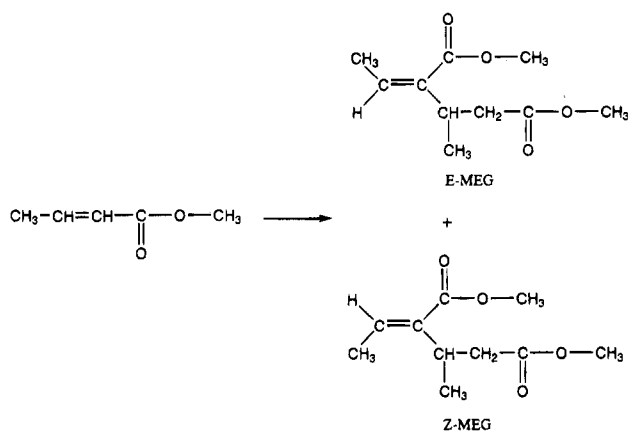

Among various types of basic catalysts, only MgO exhibits a high activity. The reasons why only MgO is active are not clear yet, but the other base catalysts such as CaO, La_2O_3, ZrO_2, KOH/Al_2O_3, and KF/Al_2O_3 show negligible activities as compared to MgO. The reaction is initiated by abstraction of allylic H of methyl crotonate by the basic site to form an allyl carbanion. The carbanion attacks a second methyl crotonate at the β-position to form the methyl diester of 3-methyl-2-vinylglutalic acid, which undergoes double bond migration to form the final product.

IV-11. The Wittig–Horner Reaction and Knoevenagel Condensation

Aldehydes react with nitriles over basic catalysts such as MgO, ZnO, and $Ba(OH)_2$ to yield the Wittig–

Horner reaction and the Knoevenagel condensation as shown below.[85]
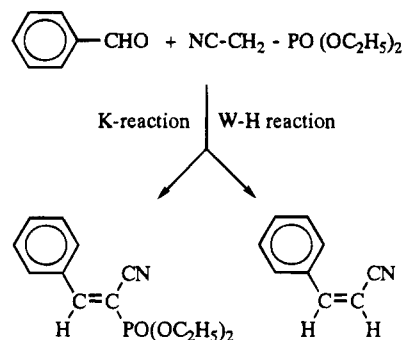
For the Knoevenagel condensation of benzaldehyde with the compounds possessing a methylene group, hydrotalcite and alkali ion-exchange zeolites[86] and alkali ion-exchange sepiolites[87] act as catalysts. For the zeolites and sepiolites, the aldol condensation which would occur as a side reaction is suppressed due to weak basic properties, and Michael addition producing bulky products is also suppressed due to the small space of the cavities where the basic sites are located. The activities of the zeolite are enhanced by replacing framework Si by Ge, which causes a change in the basic properties.[88]

IV-12. Synthesis of α,β-Unsaturated Compound by Use of Methanol

The methyl and methylene groups at the α-position of saturated ketones, esters, and nitriles are converted to vinyl groups by reactions with methanol over MgO modified by Mn ion or Cr ion.[89-93] Ueda et al. reported that acetonitrile reacts with methanol to produce acrylonitrile over Mn–MgO at the reaction temperature of 648 K.

$$CH_3CN + CH_3OH \longrightarrow CH_2{=}CHCN + H_2 + H_2O$$
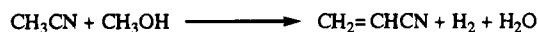
Magnesium oxide is required to be modified by addition of transition metal ions to exhibit high

Scheme 14. Formation of Acrylonitrile

Table 4. Requirements on Zeolites in O/S and O/S Transformations

reaction	basic	acidic
saturated 5-member ring + NH$_3$	−	+
saturated 5-member ring + H$_2$S	+	+
saturated 6-member ring + NH$_3$	−	++
unsaturated 5-member ring + NH$_3$	+	−
unsaturated 5-member ring + H$_2$S	+	−
saturated 5-member ring lactone + NH$_3$	+	+
saturated 5-member ring lactone + H$_2$S	+	−
saturated 6-member ring lactone + NH$_3$	−	+

the intermediate methylene anion, which is also adsorbed on the added metal ion.

Ueda et al. expanded the reaction of acetonitrile with methanol to the formations of α,β-unsaturated compounds generally expressed as follows:

$$R-CH_2Z + CH_3OH \longrightarrow R-\underset{\underset{CH_2}{\|}}{C}-Z + H_2 + H_2O$$
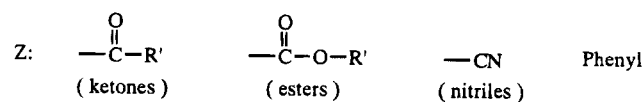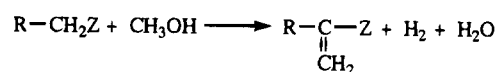
R: Alkyl, -H

IV-13. Ring Transformation

An oxygen atom in a ring position can be replaced by N or S with NH$_3$ or H$_2$S over zeolite catalysts for which the acid and base properties are adjusted by ion exchange.[94-98]

X: S, -NH

activity and selectivity for the reaction. The addition of a metal ion with an ionic radius larger than Mg^{2+} ion increases the amount of basic sites, while the addition of a metal ion with an ionic radius smaller than Mg^{2+} ion induces the surface acid sites without any appreciable change in the amount of surface basic sites. The active catalysts are obtained in the latter case.

On the basis of isotopic tracer studies for reaction mechanisms, Scheme 14 is elucidated.

The reaction mechanisms consist essentially of dehydrogenation and aldol type condensation. Methanol is dehydrogenated to form formaldehyde, which undergoes aldol condensation with acetonitrile. At first, methanol is dissociated on the basic site to form H$^+$ and CH$_3$O$^-$. The methoxy anion (CH$_3$O$^-$) is adsorbed on the added metal ion site because the metal ion is a stronger Lewis acid than Mg^{2+} ion. Then, an H$^-$ is abstracted from the methoxy anion by the metal ion to form formaldehyde. On the other hand, an H$^+$ is abstracted from acetonitrile to form

For the reaction of γ-butyrolactone and H$_2$S, the activity order is CsY > RbY > KY > NaY > LiY, which coincides with the strength of basicity. Hoelderich summarizes the relation between acid−base properties and the selectivities as given in Table 4.[99] The question as to what properties the catalysts should possess, i.e. basicity or acidity, for O/N and O/S exchange of heterocyclic compounds cannot be answered definitely. However, there is a tendency that increasing the basic properties enhances the activity and selectivity for ring transformation of O into S with H$_2$S. The basic sites that exist in the zeolite cavities should play an important role for the ring transformation reactions.

IV-14. Reactions of Organosilanes

Recently, reactions involving organosilanes have been reported to be catalyzed by heterogeneous basic catalysts. Onaka et al. reported that heterogeneous

basic catalyst such as MgO, CaO, and hydroxyapatite catalyze cyanosilylations of carbonyl compounds and unsaturated ketones like 2-cyanohexenone with cyanomethylsilane.[100,102] Basic sites interact strongly with Si in silanes so that the nucleophilicity of the silanes increases. In the cyanosilylation of unsaturated ketones, 1,2-addition products are selectively formed by use of basic catalysts, while 1,4-addition products are obtained by use of acidic catalyst such as ion-exchanged mortmorillonites.

For the formation of silane by disproportionation of trimethoxysilane, heterogeneous basic catalysts are used:[103]

$$4(CH_3O)_3SiH \rightarrow SiH_4 + 3(CH_3O)_4Si$$
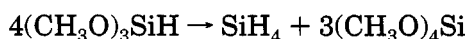
High activities were reported for hydrotalcite and alumina-supported fluorides such as KF/Al_2O_3.

V. Characteristic Features of Heterogeneous Basic Catalysts of Different Types

The catalytic properties of heterogeneous basic catalysts are closely associated with the amount and strength of the basic sites existing on the surfaces. However, the amount and strength of the basic sites are not whole measures to determine the catalytic properties. The other factors to be taken into account are not clear at present. It appears that there are characteristic features commonly observed for a certain type of heterogeneous basic catalysts. In this section, catalytic features of different types of heterogeneous catalysts are described.

V-1. Single Component Metal Oxides

Alkaline earth oxides such as MgO, CaO, SrO, and BaO are most extensively studied. They possess strong basic sites. The order of the basic strength is BaO > SrO > CaO > MgO. As described in the earlier section, the surfaces are covered with CO_2 and H_2O before pretreatment. To be active catalysts, they need pretreatment at a high temperature to remove adsorbed CO_2 and H_2O. In addition, the active sites are easily poisoned by even small amounts of impurities like CO_2 and H_2O contained in the reactants. To obtain full capabilities of alkaline earth oxides, the reaction system should be kept free of the impurities, which makes the industrial uses of the alkaline earth oxides difficult, especially at low reaction temperatures. At high reaction temperatures, the poisoning effects are reduced, and certain alkaline earth oxides show catalytic activities for the reactions from which poisons like H_2O are liberated.

One of the features of alkaline earth oxides is a high ability to abstract an H^+ from an allylic position. This feature is revealed in the double bond migration of olefinic compounds. Butene, for instance, undergoes double bond migration even at 223 K.

Rare earth oxides have been studied to a lesser extent as compared to alkaline earth oxides. The reactions for which basic sites of rare earth oxides are relevant are hydrogenation of olefins, double bond migration of olefins, aldol condensation of ketones, and dehydration of alcohols. The activity sequences of a series of rare earth oxides are shown in Figure
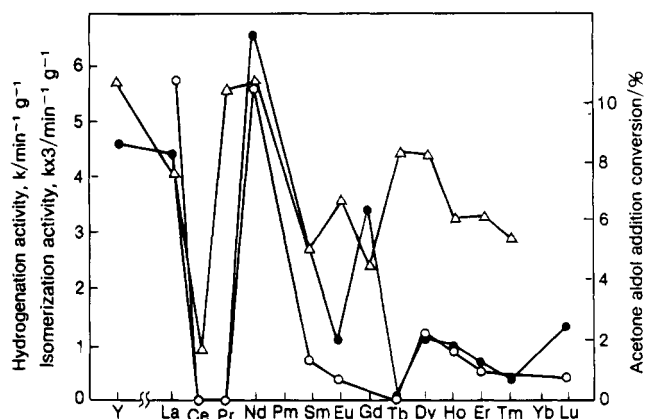
Figure 18. Catalytic activities of rare earth oxides for 1-butene isomerization (O), 1,3-butadiene hydrogenation (●), and aldol addition of acetone (△).

18 for 1-butene isomerization, 1,3-butadiene hydrogenation, and acetone aldol condensation.[104] The activity sequence is the same for 1-butene isomerization and 1,3-butadiene hydrogenation, which is different from that of aldol condensation. For the isomerization and the hydrogenation, the oxides of sesquioxide stoichiometry show activity while the oxides with metal cations of higher oxidation states are entirely inactive. The situation is different in acetone aldol condensation. The oxides with high oxidation state, CeO_2, Tb_4O_7, and Pr_6O_{11}, show considerable activity. The oxides with metal cations of oxidation state higher than 3 possess weak basic sites which are sufficient to catalyze the aldol condensation but not strong enough to catalyze hydrogenation and isomerization.

As described in the preceding section, rare earth oxides show characteristic selectivity in dehydration of alcohols. 2-Alcohols undergo dehydration to form 1-olefins. The formation of thermodynamically unstable 1-olefins contrasts with the formation of stable 2-olefins in the dehydration over acidic catalysts. The selectivity is the same as that observed for ZrO_2.

Zirconium oxide is a unique heterogeneous basic catalyst in the sense that two industrial processes have been established recently that use ZrO_2 as a catalyst. One is reduction of aromatic carboxylic acids with hydrogen to produce aldehydes.[61] The other is dehydration of 1-cyclohexylethanol to vinylcyclohexane.[48] In addition, the production of diisobutyl ketone from isobutyraldehyde has been industrialized for more than 20 years.[105] The reaction scheme for the production of diisobutyl ketone in which the Tishchenko reaction is involved is shown in Scheme 15.

One of the difficulties of most of the heterogeneous basic catalysts for industrial uses arises from rapid poisoning by CO_2 and H_2O. This is not the case with ZrO_2. Zirconium oxide retains its activity in the presence of water, which is one of the products for the reactions of carboxylic acid and 1-cyclohexylethanol.

The catalytic features of ZrO_2 are understood in terms of bifunctional acid—base properties.[49,106,107] Although the strengths of the basic and acid sites are low, a cooperative effect makes ZrO_2 function as an efficient catalyst. Because of weakly acidic and basic

Scheme 15. Formation of Ketone from Aldehyde

$$4RCH_2OH \xrightarrow{- 4H_2} 4RCHO \xrightarrow{\text{Tishchenko reaction}} 2RCH_2OOCR \xrightarrow{+ 2H_2O} \begin{array}{c} 2RCH_2OH \\ 2RCOOH \end{array}$$

$$RCOR + CO_2 + H_2O$$
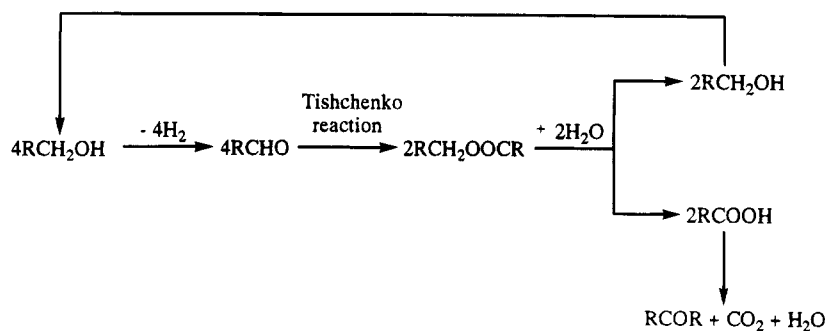
sites, the active sites are not poisoned by CO_2 and water.

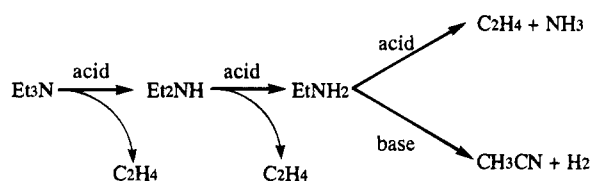Zirconium oxide shows not only basic properties but also acidic properties, depending on the reactant.[106] The acid—base bifunctionality of ZrO_2 is clearly revealed in the reaction of alkylamine to nitrile.[108] The conversion of secondary amines and tertiary amines to nitriles requires both acidic and basic sites as shown below.

$$Et_3N \xrightarrow[\downarrow C_2H_4]{acid} Et_2NH \xrightarrow[\downarrow C_2H_4]{acid} EtNH_2 \begin{array}{c} \xrightarrow{acid} C_2H_4 + NH_3 \\ \xrightarrow{base} CH_3CN + H_2 \end{array}$$

By use of acidic catalyst like $SiO_2-Al_2O_3$, ethylene and ammonia are formed. Over ZrO_2, dehydrogenation to produce nitrile occurs in preference to the formation of ethylene and ammonia.

Although ZrO_2 shows interesting catalytic properties, the structure of the active sites is still unclear. Clarification of the active sites is desired.

V-2. Zeolites

The characteristic features of zeolites result from their ion-exchange ability and specific pore structure. The acid—base properties are controlled by selecting the types of ion-exchanged cations and by the Si/Al ratio of the zeolite framework. Wide variation of acid—base properties can be achieved by ion-exchange and ion-addition, while relatively small change in acid—base properties is yielded by changing the Si/Al ratio.

To prepare basic zeolites, two approaches have been undertaken. One approach is to ion-exchange with alkali metal ions, and the other is to impregnate the zeolite pores with fine particles that can act as bases themselves. The former produces relatively weak basic sites, while the latter results in the strong basic sites.

With alkali ion-exchanged zeolites, the type of alkalis used affects the basic strength of the resulting zeolites. Effects of the alkali ions on basic strength are in the following order: $Cs^+ > Rb^+ > K^+ > Na^+ > Li^+$. the basic sites are framework oxygen. The bonding of the framework oxygen is rather covalent in nature. This causes the basic sites of ion-exchanged zeolites to be relatively weak as compared to, for example, those of alkaline earth oxides.

Table 5. Activities of Ion-Exchanged and Ion-Added Zeolites for 1-Butene Isomerization

catalyst[a]	reaction rate/mmol g^{-1} min^{-1}	
	273 K	423 K
NaX E	0	0
NaX A	0	1.1×10^{-2}
KX E	0	0
KX A	2.4×10^{-2}	7.8×10^{-2}
RbX E	0	0
RbX A	3.2×10^{-2}	1.3
CsX E	8.6×10^{-4}	1.3×10^{-1}
CsX A	1.4×10^{-1}	1.1

[a] E, ion-exchanged; A, ion-added.

Preparation of fine particles of alkali oxides inside the cavities of zeolites was developed by Hathaway and Davis.[72,109] They impregnate NaY zeolite with cesium acetate aqueous solution and calcine at 723 K to decompose cesium acetate into cesium oxide placed in the cavities. The resulting zeolite possesses basic sites stronger than those of simple ion-exchanged zeolite.

Tsuji et al. prepared the zeolites containing a series of alkali metal ions in excess of the ion-exchanged capacities and compared their catalytic activities and basic sites with simply ion-exchanged zeolites. TPD plots of adsorbed carbon dioxide are shown in Figure 9. The TPD peaks appear at higher temperatures for "ion-added" zeolites than for ion-exchanged zeolites, indicating generation of new basic sites that are stronger than sites of ion-exchanged zeolites.

The results of the catalytic activities of the ion-added zeolites and the ion-exchanged zeolites for 1-butene isomerization are summarized in Table 5.[17,110] Except for CsX, ion-exchanged zeolites did not exhibit any activities at 273 K and 423 K. The ion-added zeolites showed considerable activities, and the order of the activities for different alkali ions was Cs > Rb > K > Na.

Zeolites often collapse during preparation procedures. Yagi et al. prepared Cs ion-added zeolites to establish the preparative conditions to retain the zeolite framework during preparative procedures.[111] It was found that the crystalline structures of zeolites, in particular alkali ion-added zeolites, are easily destroyed by exposure to water vapor at high temperatures and that zeolites of high Si/Al ratio are unstable to alkali treatment.

Besides alkali metal oxides, the fine particles of MgO were placed in the zeolite cavities.[110] The resulting zeolites also showed strong basic properties, though the basic sites on the fine particles of MgO

are not as strong as those of bulk MgO. The ionicity of the Mg−O bond is reduced for a fine particle of MgO as compared to bulk MgO, and therefore, the basic strength of the O^{2-} ion is reduced. The dependence of the particle size on the strength of basic site was studied for ultrafine MgO particles by Itoh et al.[112] It was also concluded that smaller particles exhibit weaker basicity.

One of the important objects for preparation of basic zeolites is to realize the shape selectivity in base-catalyzed reactions. Corma et al. reported the shape selectivity of alkali ion-exchanged zeolites in the reaction of benzaldehyde with ethyl cyanoacetate.[113] Lasperas et al. prepared zeolite containing cesium oxide in the cavities by the "postsynthetic method", which is similar to the methods by Harthaway and Davis[72] and Tsuji et al.[17,110] The reaction of benzaldehyde with ethyl cyanoacetate proceeded as shown below.[114,115]
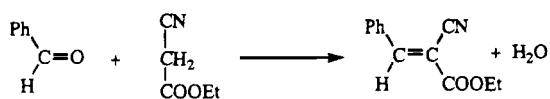
Knoevenagel condensation
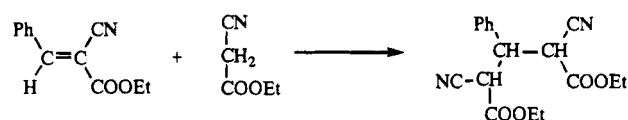
Michael addition

Knoevenagel condensation proceeded, but the product did not undergo the following Michael addition because of the limited space in the zeolite cavities.

Tsuji et al. reported the shape selectivity of the zeolite containing MgO.[110] Nonsupported MgO catalyzes double bond migrations of both 1-butene and allylbenzene, while the zeolite containing MgO in the cavities catalyzes the former but fails to catalyze the latter.

The studies of basic zeolites, in particular, those of strongly basic zeolites have started quite recently. To reveal the potential of basic zeolites, establishment of preparative methods, identification of basic sites, and application of the basic zeolites to a wide variety of the base-catalyzed reactions are required.

V-3. Basic Catalysts of the Non-Oxide Type

Most of heterogeneous basic catalysts are in the form of oxides. The basic sites are O^{2-} ions with different environments depending on their type. If the basic sites are constituted by elements other than O^{2-}, the catalysts are expected to show catalytic properties different than those of the catalysts of the oxide form.

Potassium fluoride supported on alumina (KF/Al_2O_3) was introduced by Clark[116] and by Ando and Yamawaki[117,118] as a fluorinating reagent and a base catalyst. As a base catalyst, KF/Al_2O_3 has been applied to a number of organic reactions. The reactions for which KF/Al_2O_3 acts as a catalyst include Michael additions,[82,83,119,120] Wittig−Honner reactions,[121,122] Knoevenagel condensations,[121,122] Darzen condensations,[81,121] condensation of phenyl acetylene
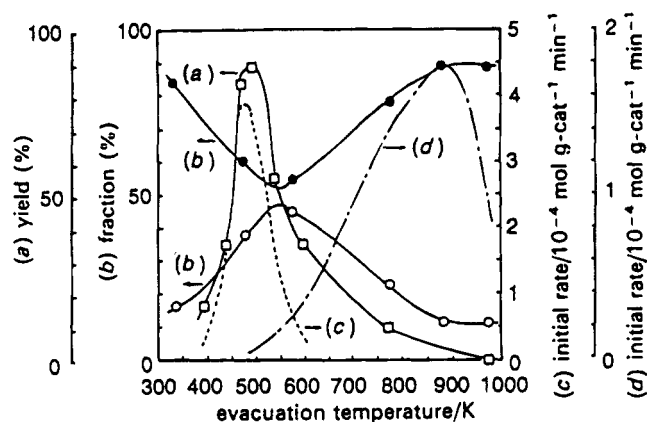

Figure 19. Fraction of Yb^{3+} (●) and Yb^{2+} (○) plotted against evacuation temperature and the catalytic activities of Yb/Na-Y for (- -) 1-butene isomerization, (− • −) ethylene hydrogenation, and (□) Michael reaction of cyclopent-2-enone with dimethyl malonate. 1-Butene isomerization was carried out at 273 K over Yb/NaY. Ethylene hydrogenation was carried out at 273 K over Yb/LY. Michael reaction was carried out at 323 K over Yb/NaY. (Reprinted from 133. Copyright 1993 Chemical Society of London.)

with benzaldehyde,[124] alkylations at C, O, N, and S with aldehydes and dimethyl sulfate,[117,125−127] and disproportionation of alkylsilanes.[103]

In contrast to many applications to organic syntheses as a base catalyst, KF/Al_2O_3 has not been studied extensively for the surface properties, and the structures of basic sites have not been clarified yet. At the beginning, the basic sites were considered to be F^- ions dispersed on the alumina support. Insufficient coordination only with surface OH groups may result in the formation of active F^- ions. This was supported by ^{19}F MASNMR.[128−130]

On the other hand, it was proposed on the basis of IR and XRD studies that the basic sites originate from KOH and/or aluminate produced by the following reactions:[129,131]

$$12KF + Al_2O_3 + 3H_2O \rightarrow 2K_3AlF_6 + 6KOH$$

$$6KF + 2Al_2O_3 \rightarrow 3K_3AlF_6 + 3KAlO_2$$
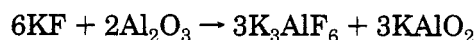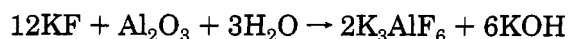
Taking account of the above results and the results of titrating the water soluble base on the surface together with the results of IR study, thermogravimetry, and SEM, Ando et al. concluded that there are three basic species or mechanisms of the appearance of the basicity on the surface of KF/Al_2O_3.[130,132] These are (i) well-dispersed and incompletely coordinated F^- ions, (ii) [Al−O^-] ions which generate OH^- ions when water is present, and (iii) cooperation of F^- and [Al−OH] which can behave as an in situ-generated base during the course of the reaction.

For the other catalysts of the non-oxide type, Baba et al. prepared low-valent lanthanide species introduced into zeolite cavities.[133,134] They impregnated K−Y with Yb and Eu dissolved into liquid ammonia followed by thermal activation. The variations of the catalytic activities of the Yb/K−Y catalyst as a function of the thermal activation temperature are shown in Figure 19 for 1-butene isomerization, ethylene hydrogenation, and Michael addition of cyclopenten-2-one with dimethyl malonate.[133]

The chemical states of Yb were studied by TPD, IR, XAFS, and XPS as a function of evacuation temperature. The states of Yb changed from Yb(II, III) amides, Yb(II, III) imides, to Yb(III) nitride as follows:

$$Yb(NH_2)_3 \rightarrow YbNH + NH_3 + {}^1/_2 N_2 + H_2$$

$$Yb(NH_2)_2 \rightarrow YbNH + NH_3$$

and

$$2YbNH \rightarrow 2YbN + H_2$$
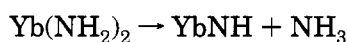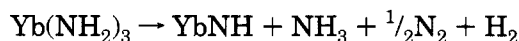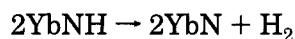
As for the catalytically active sites, it was concluded that the Yb(II) imide species catalyze 1-butene isomerization and the Michael addition and that the Yb(III) nitride species catalyzes ethylene hydrogenation.

In the above reactions, characteristic features which distinguish the non-oxide catalysts from the metal oxides are not obvious. However, it is expected that the features will become apparent for certain base-catalyzed reactions if the applications of the non-oxide catalysts to various kinds of reactions are expanded.

V-4. Heterogeneous Superbasic Catalysts

To activate a reactant under mild conditions, a catalyst possessing very strong basic sites is desired to be prepared. There have been some attempts to prepare those superbasic catalysts.

Suzukamo et al. prepared a superbasic catalyst by addition of alkali hydroxides to alumina followed by further addition of alkali metals.[41] To a calcined alumina, sodium hydroxide was added at 583–593 K with stirring under a nitrogen stream. In 3 h, sodium metal was added and the mixture was stirred for another 1 h at the same temperature to give a pale blue solid. The resulting catalyst possesses basic sites stronger than $H_- = 37$ and catalyzes various base-catalyzed reactions such as double bond migrations of 5-vinylbicyclo[2.2.1]hept-2-ene to 5-ethylidenebicyclo[2.2.1]hept-2-ene at the reaction temperature 243–373 K, 2,3-dimethylbut-1-ene to 2,3-dimethylbut-2-ene at 293 K, and safrol to isosafrol at 293 K and side chain alkylations of alkylbenzenes at the reaction temperature 293–433 K. The former two reactions are initiated by abstraction of an H^+ from the tertiary carbon in the molecules to form tertiary carbanions. Because tertiary carbanions are unstable, the abstraction of an H^+ from a tertiary carbon requires a strong basic site.

Ushikubo et al. prepared a superbasic catalyst by addition of metallic sodium to MgO.[135] Magnesium oxide was pretreated at a high temperature and mixed with NaN_3. The mixture was heated at 623 K to decompose NaN_3 to evolve metallic sodium vapor to which MgO was exposed. The resulting catalyst acted as an efficient catalyst for decomposition of methyl formate to CO and methanol. The activity was much higher than that of MgO. Although the basic strength of Na-added MgO was not compared with that of MgO, the high activity of Na-added MgO for the decomposition of methyl formate appears to be due to the enhancement of basic strength caused by the addition of Na to MgO.

VI. Concluding Remarks

Heterogeneous basic catalysts have been investigated for almost 40 years during which a number of reactions have been found to proceed on the basic catalysts. Nevertheless, the reactions for which heterogeneous basic catalysts have been used are only a part of a great number of organic reactions. Use of heterogeneous basic catalysts in organic syntheses has been increasing in recent years. There should be many reactions which heterogeneous basic catalysts can efficiently promote, but have not been used for. One reason for the limited use of heterogeneous basic catalysts arises from a rapid deactivation while being handled under the atmosphere; the catalysts should be pretreated at high temperatures and handled in the absence of air prior to use for the reaction. If this care is taken, heterogeneous catalysts should promote a great number of reactions.

It was found that some of the reactions specifically proceed on the heterogeneous basic catalysts. The catalytic actions of heterogeneous basic catalysts are not simple copies of those of homogeneous basic catalysts, though it is not clearly understood where the features of heterogeneous basic catalysts originate from. To clarify this point, characterizations of the surface sites together with elucidation of the reaction mechanisms occurring on the surfaces should be extended.

Although the theoretical calculations of the surface sites and the reaction mechanisms are not described in this article, there have been efforts on these points.[136–141] The results of the quantum chemical calculations explain well the experimental results, and give us valuable information about the heterogeneous basic catalysis. Unfortunately, the theoretical calculations have been done only for the MgO catalyst. An attempt to calculate the other catalyst systems is highly desirable.

The methods of preparing heterogeneous catalysts and the characterizations of the surfaces have been developed. Keen insight into the surface reaction mechanisms and the functions required for the reactions together with the accumulation of the heterogeneous base-catalyzed reactions will enable to design the heterogeneous basic catalysts active for desired reactions.

References

(1) Pines, H.; Veseley, J. A.; Ipatieff, V. N. *J. Am. Chem. Soc.* **1955**, 77, 6314.
(2) Kokes, R. J.; Dent, A. L. *Advan. Catal.* **1972**, 22, 1.
(3) Kokes, R. J. *Proceedings of the 5th International Congress of Catalysis* Miami Beach, FL, 1972; p 1.
(4) Hattori, H.; Yoshii, N.; Tanabe, K. *Proceedings of the 5th International Congress on Catalysis*, Miami Beach, FL, 1972; p 233.
(5) Yashima, T.; Sato, K.; Hayasaka, T.; Hara, N. *J. Catal.* **1972**, 26, 303.
(6) Tanabe, K.; Misono, M.; Ono, Y.; Hattori, H. *New Solid Acids and Bases*; Kodansha (Tokyo)–Elsevier (Amsterdam, Oxford, New York, Tokyo), 1989; p 30.
(7) Hattori, H.; Maruyama, K.; Tanabe, K. *J. Catal.* **1976**, 44, 50.

(8) Tanabe, K.; Misono, M.; Ono, Y.; Hattori, H. *New Solid Acids and Bases*; Kodansha (Tokyo)−Elsevier (Amsterdam, Oxford, New York, (Tokyo), 1989; p 39.

(9) Coluccia, S.; Tench, A. J. *Proceedings of the 7th International Congress on Catalysis* Tokyo, Japan, 1980; p 1160.

(10) Fukuda, Y.; Hattori, H.; Tanabe, K. *Bull. Chem. Soc. Jpn.* **1978**, *51*, 3151.

(11) Imizu, Y.; Sato, K.; Hattori, H. *J. Catal.* **1981**, *71*, 64.

(12) Utiyama, M.; Hattori, H.; Tanabe, K. *J. Catal.* **1978**, *4*, 237.

(13) Hammett, L. P. *Physical Organic Chemistry*; McGraw-Hill: New York, 1940; Chapter IX.

(14) Paul, M. A.; Long, F. A. *Chem. Rev.* **1957**, *57*, 1.

(15) Take, J.; Kikuchi, N.; Yoneda, Y. *J. Catal.* **1971**, *21*, 164.

(16) Zhang, G.; Hattori, H.; Tanabe, K. *Appl. Catal.* **1988**, *36*, 189.

(17) Tsuji, H.; Yagi, F.; Hattori, H. *Chem. Lett.* **1991**, 1881.

(18) Nelson, R. L.; Hale, J. W. *Disc. Faraday Soc.* **1958**, *52*, 77.

(19) Tench, A. J.; Pott, G. T. *Chem. Phys. Lett.* **1974**, *26*, 590.

(20) Zecchina, A.; Lofthouse, M. G.; Stone, F. S. *J. Chem. Soc. Faraday Trans. I*, **1975**, *71*, 1476.

(21) Coluccia, S.; Tench, A. J.; Segall, R. L. *J. Chem. Soc. Faraday 1* **1978**, *75*, 1769.

(22) Stone, F. S.; Zecchina, A. *proceedings of the 6th International Congress on Catalysis* London, 1976, p 162.

(23) Ito, T.; Kuramoto, M.; Yoshida, M.; Tokuda, T. *J. Phys. Chem.* **1983**, *87*, 4411.

(24) Ito, T.; Murakami, T.; Tokuda, T. *J. Chem. Soc. Trans. Faraday I*, **1983**, *79*, 913.

(25) Okamoto, Y.; Ogawa, M.; Maezawa, A.; Imanaka, T. *J. Catal.* **1988**, *112*, 427.

(26) Huang, M.; Adnot, A.; Kaliaguine, S. *J. Catal.* **1992**, *137*, 322.

(27) Barthomeuf, D. *J. Phys. Chem.* **1978**, *55*, 138.

(28) Fukuda, Y.; Tanabe, K. *Bull. Chem. Soc. Jpn.* **1973**, *46*, 1616.

(29) Evans, J. V.; Whateley, T. L. *Trans. Faraday Soc.* **1967**, *63*, 2769.

(30) Barthomeuf, D. *Stud. Surf. Sci. Catal.* **1991**, *65*, 157.

(31) Yanagisawa, Y.; Shimodama, H.; Ito, A. *J. Chem. Soc. Chem. Commun.* **1992**, 610.

(32) Shishido, T.; Tsuji, H.; Gao, Y.; Hattori, H.; Kita, H. *React. Kinet. Catal. Lett.* **1993**, *51*, 75.

(33) Tuji, H.; Shishido, T.; Okamura, A.; Gao, Y.; Hattori, H.; Kita, H. *J. Chem. Soc. Faraday Trans.* **1994**, *90*, 803.

(34) Hattori, H. *Stud. Surf. Sci. Catal.* **1993**, *78*, 35.

(35) Tsuchiya, S. *Acid-Base Catalysis*; Kodansha (Tokyo)−VCH (Basel, Cambridge, New York, Weinheim), 1989; p 169.

(36) Hightower, J. W.; Hall, K. W. *J. Am. Chem. Soc.* **1967**, *89*, 778.

(37) Satoh, A.; Hattori, H. *J. Catal.* **1976**, *45*, 36.

(38) Hattori, H.; Itoh, M.; Tanabe, K. *J. Catal.* **1976**, *41*, 46.

(39) Hattori, H.; Tanabe, K.; Hayano, K.; Shirahama, H.; Matsumoto, T. *Chem. Lett.* **1979**, 133.

(40) Shimazu, K.; Tanabe, K.; Hattori, H. *J. Catal.* **1977**, *45*, 302.

(41) Suzukamo, G.; Fukao, M.; Hibi, T.; Chikaishi, K. *Acid-Base Catalysis*; Kodansha (Tokyo)−VCH (Basel, Cambridge, New York, Weinheim), 1989; p 405.

(42) Suzukamo, G.; Fukao, M.; Minobe, M. *Chem. Lett.* **1987**, 585.

(43) Hattori, A.; Hattori, H.; Tanabe, K. *J. Catal.* **1980**, *65*, 246.

(44) Matsuhashi, H.; Hattori, H. *J. Catal.* **1984**, *85*, 457.

(45) Lundeen, A. J.; van Hoozen, R. *J. Org. Chem.* **1967**, *32*, 3386.

(46) Tomatsu, T.; Yoneda, H.; Ohtsuka, H. *Yukagaku*, **1968**, *17*, 236.

(47) Thomke, K. *Proceedings of the 6th International Congress on Catalysis* London, UK, 1976; p 303.

(48) Yamaguchi, T.; Sasaki, H.; Tanabe, K. *Chem. Lett.* **1976**, 677.

(49) Takahashi, K.; Hibi, T.; Higashio, Y.; Araki, M. *Shokubai (Catalyst)* **1993**, *35*, 12.

(50) Ueshima, M.; Yano, H.; Hattori, H. *Sekiyu Gakkaisi (J. Jpn. Petroleum Inst.)* **1992**, *35*, 362.

(51) Hattori, H.; Tanaka, Y.; Tanabe, K. *J. Am. Chem. Soc.* **1976**, *98*, 4652.

(52) Tanaka, Y.; Imizu, Y.; Hattori, H.; Tanabe, K. *Proceedings of the 7th International Congress on Catalysis* Tokyo, Japan 1980; p 1254.

(53) Imizu, Y.; Hattori, H.; Tanabe, K. *J. Catal.* **1979**, *56*, 303.

(54) Imizu, Y.; Hattori, H.; Tanabe, *J. Chem. Soc. Chem. Commun.* **1978**, 1091.

(55) Nakano, Y.; Yamaguchi, T.; Tanabe, K. *J. Catal.* **1983**, *80*, 307.

(56) Imizu, Y.; Sato, K.; Hattori, H. *J. Catal.* **1982**, *76*, 235.

(57) Hattori, H.; Wang, G. *Proceedings of the 8th International Congress on Catalysis* Berlin, Germany 1984; p III-219.

(58) Wang, G.; Hattori, H. *J. Chem. Soc. Faraday Trans. 1* **1984**, *80*, 1039.

(59) Yamaguchi, T.; Hightower, J. W. *J. Am. Chem. Soc.* **177**, *99*, 4201.

(60) Shima, H.; Yamaguchi, T. *J. Catal.* **1984**, *90*, 160.

(61) Yokoyama, T.; Setoyama, T.; Fujita, N.; Nakajima, M.; Maki, T.; Fukii, K. *Appl. Catal. A* **1992**, *88*, 149.

(62) Yokoyama, T.; Setoyama, T.; Nakajima, M.; Fujita, N.; Maki, T. *Acid-Base Catalysis II*; Kodansha (Tokyo)−Elsevier (Amsterdam, Oxford, New York, Tokyo), 1994; p 47.

(63) Kakuno, Y.; Hattori, H. *J. Catal.* **1984**, *85*, 509.

(64) Shibagaki, M.; Takahashi, K.; Matsushita, H. *Bull. Chem. Soc. Jpn.* **1988**, *61*, 3283.

(65) Takahashi, K.; Shibagaki, M.; Matsushita, H. *Bull. Chem. Soc. Jpn.* **1989**, *62*, 2353.

(66) Takahashi, K.; Shibagaki, M.; Kuno, H.; Kawakami, H.; Matsushita, H. *Bull. Chem. Soc. Jpn.* **1989**, *62*, 1333.

(67) Shabtai, J.; Lazer, R.; Biron, E. *J. Mol. Catal.* **1984**, *27*, 35.

(68) Suzuka, H.; Hattori, H. *Appl. Catal.* **1989**, *48*, L7.

(69) Suzuka, H.; Hattori, H. *J. Mol. Catal.* **1990**, *63*, 371.

(70) Ito, H.; Miyamoto, A.; Murakami, Y. *J. Catal.* **1980**, *64*, 284.

(71) Miyamoto, A.; Iwamoto, S.; Agusa, K.; Inui, T. *Acid-Base Catalysis*; Kodansha (Tokyo)−VCH (Basel, Cambridge, New York, Weinheim), 1989; p 497.

(72) Hathaway, P. E.; Davis, M. E. *J. Catal.* **1989**, *119*, 497.

(73) Zhang, G.; Hattori, H.; Tanabe, K. *Appl. Catal.* **1988**, *36*, 189.

(74) Zhang, G.; Hattori, H.; Tanabe, K. *Appl. Catal.* **1988**, *40*, 183.

(75) Yashima, T.; Suzuki, H.; Hara, N. *J. Catal.* **1974**, *33*, 486.

(76) Chu, P.; Kuehl, G. W. US Patent, 4,605,787, 1986.

(77) Weirzchowski, P. T.; Zatorski, L. W. *Catal. Lett.* **1991**, *9*, 411.

(78) Suzuki, E.; Idemura, S.; Ono, Y. *Chem. Lett.* **1987**, 1843.

(79) Tanabe, K.; Saito, K. *J. Catal.* **1974**, *35*, 274.

(80) Garcia-Raso, A.; Garcia-Raso, J.; Campaner, B.; Mestres, R.; Sinisterra, J. V. *Synthesis* **1982**, 1037.

(81) Yamawaki, J.; Kawate, T.; Ando, T.; Hanafusa, T. *Bull. Chem. Soc. Jpn.* **1983**, *56*, 1885.

(82) Campelo, J. M.; Climent, M. S.; Marinas, J. M. *React. Kinet. Catal. Lett.* **1992**, *47*, 7.

(83) Laszlo, P.; Peuneteau, P. *Tetrahedron Lett.* **1983**, *22*, 2645.

(84) Kabashima, H.; Tsuji, H.; Hattori, H.; Kita, H. Submitted.

(85) Sinisterra, J. V.; Mouloungui, Z.; Marinas, M. *J. Colloid Interface Sci.* **1987**, *115*, 520.

(86) Corma, A.; Fornas, V.; Martin-Aranda, R. H.; Garcia, H.; Promo, J. *Appl. Catal.* **1990**, *59*, 237.

(87) Corma, A.; Martin-Aranda, Sanchez, F. *J. Catal.* **1990**, *126*, 192.

(88) Texier-Boullet, F.; Faucand, A. *Tetrahedron Lett.* **1982**, *23*, 4927.

(89) Ueda, W. *Sekiyu Gakkaishi (J. Jpn. Petroleum Inst.)* **1933**, *36*, 421.

(90) Kurokawa, H.; Kato, T.; Ueda, W.; Morikawa, Y.; Moro-oka, Y.; Ikawa, T. *J. Catal.* **1990**, *126*, 199.

(91) Kurokawa, H.; Kato, T.; Kuwabara, T.; Ueda, W.; Morikawa, Y.; Moro-oka, Y.; Ikawa, T. *J. Catal.* **1991**, *126*, 208.

(92) Kurokawa, H.; Ueda, W.; Morikawa, Y.; Moro-oka, Y.; Ikawa, T. *Acid-Base Catalysis*; Kodansha (Tokyo)−VCH (Basel, Cambridge, New York, Weinheim), 1989; p 93.

(93) Ueda, W.; Ohowa, H.; Iwasaki, K.; Kuwabara, T.; Ohshida, T.; Morikawa, Y. *Acid-Base Catalysis II*; Kodansha (Tokyo)−Elsevier (Amsterdam, Oxford, New York, Tokyo) 1994; p 35.

(94) Ono, Y. *Heterocycle* **1981**, *16*, 1755.

(95) Ono, Y. *Stud. Surf. Sci. Catal.* **1980**, *5*, 19.

(96) Ono, Y.; Mori, T.; Hatada, K. *Acta Phys. Chem.* **1978**, *24*, 233.

(97) Venuto, P. B.; Landis, P. S. *Adv. Catal.* **1968**, *18*, 259.

(98) Ono, Y.; Takeyama, Y.; Hatada, K.; Keii, T. *Ind. Eng. Chem. Prod. Res. Dev.* **1976**, *5*, 180.

(99) Hoelderich, W. F. *Acid-Base Catalysis*; Kodansha (Tokyo)−VCH (Basel, Cambridge, New York, Weinheim), 1989; p 1.

(100) Onaka, M.; Higuchi, K.; Sugita, K.; Izumi, Y. *Chem. Lett.* **1989**, 1393.

(101) Higuchi, K.; Onaka, M.; Izimi, Y. *J. Chem. Soc. Chem. Commun.* **1991**, 1035.

(102) Sugita, K.; Ohta, A.; Onaka, M.; Izumi, Y. *Chem. Lett.* **1990**, 481.

(103) Nomoto, Y.; Suzuki, E.; Ono, Y. *Acid-Base Catalysis II*; Kodansha (Tokyo)−Elsevier (Amsterdam, Oxford, New York, Tokyo) 1994; p 447.

(104) Hattori, H.; Kumai, H.; Tanaka, K.; Zhang, G.; Tanabe, K. *Proc. 8th National Symposium on Catalysis* Sindri, India, 1987; p 243.

(105) Koga, I. *Yuki Gouseikagaku* **1975**, *33*, 702.

(106) Yamaguchi, T. *Sekiyu Gakkaishi (J. Jpn. Petroleum Inst.)* **1993**, *36*, 250.

(107) Tanabe, T. *Proceedings of the 8th International Congress on Catalysis*, Calgary, Canada 1988; Vol. 5, p 85.

(108) Xu, B.; Yamaguchi, T.; Tanabe, K. *Appl. Catal.* **1990**, *64*, 41.

(109) Dart, C. B.; Davis, M. E. *Catal. Today* **1994**, *19*, 151.

(110) Tsuji, H.; Yagi, F.; Hattori, H.; Kita, H. *Proceedings of the 10th International Congress on Catalysis*, Budapest, Hungary, 1992, p 1171.

(111) Yagi, F.; Tsuji, H.; Hattori, H.; Kita, H. *Acid-Base Catalysis II*; Kodansha (Tokyo)−Elsevier (Amsterdam, Oxford, New York, Tokyo), 1994; p 349.

(112) Itoh, H.; Utamapanya, S.; Stark, J. V.; Klabunde, K. J.; Schlup, J. *Chem. Mater.* **1993**, *5*, 71.

(113) Corma, A.; Martin-Aranda, R. M. *J. Catal.* **1990**, *130*, 130.

(114) Lasperas, M.; Cambon, H.; Brunel, D.; Rodriguez, I.; Geneste, P. *Microporous Mater.* **1993**, *1*, 343.

(115) Rodriguez, I.; Cambon, H.; Brunel, D.; Lasperas, M.; Geneste, P. *Stud. Surf. Sci.* **1993**, *78*, 623.

(116) Clark, J. H. *Chem. Rev.* **1980**, *80*, 429.

(117) Yamawaki, J.; Ando, T. *Chem. Lett.* **1979**, 45.

(118) Ando, T.; Yamawaki, J. *Yukigosei Kyokaishi (J. Org. Syn. Inst.)* **1981**, *39*, 14.

(119) Clark, J. H.; Cork, D. G.; Robertson, M. S. *Chem. Lett.* **1983**, 1145.

(120) Villemin, D. *J. Chem. Soc. Chem. Commun.* **1983**, 1092.

(121) Villemin, D. *Chem. Ind.* (London) **1985**, 166.

(122) Texier-Bullet, F.; Villemin, D.; Licard, M.; Mison, H.; Foucaud, A. *Tetrahedron* **1985**, *41*, 1259.

(123) Villemin, D.; Rocha, R. *Tetrahedron* **1986**, *27*, 1789.

(124) Villemin, D.; Richard, M. *Tetrahedron Lett.* **1984**, *75*, 1059.

(125) Yamawaki, J.; Ando, T.; Hanafusa, T. *Chem. Lett.* **1981**, 1143.

(126) Ando, T.; Yamawaki, J.; Kawate, T.; Sumi, S.; Hanafusa, T. *Bull. Chem. Soc. Jpn.* **1982**, *55*, 2504.

(127) Elisabeth, A. E.; Schmittiling, E. A.; Sawyer, J. S. *J. Org. Chem.* **1993**, *58*, 3229.

(128) Clark, J. H.; Goodman, E. M.; Smith, D. K.; Brown, S. J.; Miller, J. M. *J. Chem. Soc. Chem. Commun.* **1986**, 657.

(129) Duke, C. V. A.; Miller, J. M.; Clark, J. H.; Kybett, A. P. *J. Mol. Catal.* **1990**, *62*, 233.

(130) Ando, T.; Clark, J. H.; Cork, D. G.; Hanafusa, T.; Ichihara, J.; Kimura, T. *Tetrahedron Lett.* **1987**, *28*, 1421.

(131) Weinstock, L. M.; Stevenson, J. M.; Tomeliui, S. A.; Pan, S. H.; Utne, T.; Jobson, R. B.; Reinfold, F. *Tetrahedron Lett.* **1986**, *27*, 3845.

(132) Ando, T. *Acid-Base Catalysis II*; Kodansha (Tokyo)—Elsevier (Amsterdam, Oxford, New York, Tokyo), 1994; p 9.

(133) Baba, T.; Kim, G. J.; Ono, Y. *J. Chem. Soc. Faraday Trans.* **1993**, *88*, 891.

(134) Baba, T.; Hikita, S.; Koide, R.; Ono, Y.; Hanada, T.; Tanaka, T.; Yoshida, S. *J. Chem. Soc. Faraday Trans.* **1993**, *89*, 3177.

(135) Ushikubo, T.; Hattori, H.; Tanabe, K. *Chem. Lett.* **1984**, 649.

(136) Kawakami, H.; Yoshida, S. *J. Chem. Soc. Faraday Trans. 2* **1984**, *80*, 921.

(137) Fujioka, H.; Yamabe, S.; Yanagisawa, Y.; Matsumura, K.; Huzimura, R. *Surf. Sci.* **1985**, *149*, L53.

(138) Kobayashi, H.; Yamaguchi, M.; Ito, T. *J. Phys. Chem.* **1990**, *94*, 7206.

(139) Ito, T.; Tashiro, T.; Kawasaki, M.; Toi, T.; Kobayashi, H. *J. Phys. Chem.* **1991**, *95*, 4477.

(140) Sawabe, K.; Koga, N.; Morokuma, K. *J. Chem. Phys.* **1992**, *97*, 6871.

(141) Kobayashi, H.; Salahub, D. S.; Ito, T. *Acid-Base Catalysis II*; Kodansha (Tokyo)—Elsevier (Amsterdam, Oxford, New York, Tokyo), 1994; p 207.